

General Disclaimer

One or more of the Following Statements may affect this Document

- This document has been reproduced from the best copy furnished by the organizational source. It is being released in the interest of making available as much information as possible.
- This document may contain data, which exceeds the sheet parameters. It was furnished in this condition by the organizational source and is the best copy available.
- This document may contain tone-on-tone or color graphs, charts and/or pictures, which have been reproduced in black and white.
- This document is paginated as submitted by the original source.
- Portions of this document are not fully legible due to the historical nature of some of the material. However, it is the best reproduction available from the original submission.

**NASA TECHNICAL
MEMORANDUM**

NASA TM X-71785

NASA TM X-71785

(NASA-TM-X-71785) PRELIMINARY STUDY OF THE
FUEL SAVING POTENTIAL OF REGENERATIVE
TURBOFANS FOR COMMERCIAL SUBSONIC TRANSPORTS
(NASA) 47 p HC \$3.75 CSCL 21E

N75-30178

G3/07 34281
Unclas

**PRELIMINARY STUDY OF THE FUEL SAVING
POTENTIAL OF REGENERATIVE TURBOFANS
FOR COMMERCIAL SUBSONIC TRANSPORTS**

**by Gerald A. Kraft
Lewis Research Center
Cleveland, Ohio 44135
August 1975**

1. Report No. NASA TM X-71785	2. Government Accession No.	3. Recipient's Catalog No.	
4. Title and Subtitle PRELIMINARY STUDY OF THE FUEL SAVING POTENTIAL OF REGENERATIVE TURBOFANS FOR COMMERCIAL SUBSONIC TRANSPORTS		5. Report Date	
		6. Performing Organization Code	
7. Author(s) Gerald A. Kraft		8. Performing Organization Report No. E-8450	
		10. Work Unit No.	
9. Performing Organization Name and Address Lewis Research Center National Aeronautics and Space Administration Cleveland, Ohio 44135		11. Contract or Grant No.	
		13. Type of Report and Period Covered Technical Memorandum	
12. Sponsoring Agency Name and Address National Aeronautics and Space Administration Washington, D. C. 20546		14. Sponsoring Agency Code	
15. Supplementary Notes			
16. Abstract <p>The fuel savings potential of regenerative turbopumps was calculated and compared with that of a reference turbopump for use in an advanced subsonic transport. The technology of all the engines was considerably advanced and could not be expected to be ready for commercial service before the mid 1980's. At the design altitude of 10.67 km and Mach 0.80, the turbine-inlet-temperature of the regenerative turbopump was fixed at 1700 K while the overall pressure ratio was varied from 10 to 20. The fan pressure ratio was fixed at 1.6 and the bypass ratio varied from 8 to 10. The heat exchanger design parameters such as pressure drop and effectiveness varied from 4 to 8 percent and from 0.80 to 0.90, respectively. The study indicated a fuel savings due to regeneration of 4.1 percent and no change in takeoff gross weight. The change in direct operating cost ranged from 6 percent worse to 3.7 percent better depending on the fuel cost and the cost of the regenerative turbopump engine.</p>			
17. Key Words (Suggested by Author(s))		18. Distribution Statement Unclassified - unlimited	
19. Security Classif. (of this report) Unclassified	20. Security Classif. (of this page) Unclassified	21. No. of Pages	22. Price*

PRELIMINARY STUDY OF THE FUEL SAVING POTENTIAL OF REGENERATIVE
TURBOFANS FOR COMMERCIAL SUBSONIC TRANSPORTS

by Gerald A. Kraft
Lewis Research Center

SUMMARY

0548-
The fuel savings potential of a regenerative turbofan was calculated and compared with that of a reference turbofan for use in an advanced subsonic transport. The technology of all the engines was considerably advanced and could not be expected to be ready for commercial service before the mid-1980's. All the engines were designed for a cruise altitude of 10.67 kilometers (35 000 ft) and Mach 0.80. The reference turbofan had an overall pressure ratio of 40, a fan pressure ratio of 1.6, a bypass ratio of 10.4, and a turbine inlet temperature of 1620 K (2910° R). The regenerative turbofans had overall pressure ratios of 10 to 20, a fan pressure ratio of 1.6, bypass ratios of 8 to 10 and a turbine inlet temperature of 1700 K (3060° R). The heat exchanger was a rotary drum type using a ceramic matrix. The effectiveness was varied from 0.80 to 0.90 and the pressure drop from 4 to 8 percent. In addition, a total of 4 percent pressure drop was assumed in the air ducts used in conjunction with the heat exchanger.

The mission called for a payload of 18 144 kilograms (40 000 lb) to be carried a range of 5500 kilometers (3000 n mi). As gross weight changed, wing, landing gear, and engine weight varied while the fuselage and wing loading were fixed. The drag due to the changing propulsion system and wing size was taken into account.

The reference turbofan in this study used about 22 percent less fuel than a current (bypass ratio 5 to 6) turbofan if used on the same aircraft. The results of this study indicate that, relative to the reference turbofan, the regenerative turbofan could save 4.1 percent in fuel and about break even in takeoff gross weight. The change in direct operating cost ranged from 6 percent worse to 3.7 percent better depending on the fuel cost and the cost of the regenerative turbofan.

INTRODUCTION

Current aircraft are totally dependent on the oil supply for their fuels, and United States civil aircraft now use about 3.8 percent of all the oil used in the United States. Reference 1 projects that by 1984 the United States Certified Air Carriers will double their revenue passenger miles. In the same time, the jet fuel used by these carriers is estimated to increase by 50 percent. New fuel-conservative aircraft could re-

duce this fuel demand substantially. Numerous studies of such aircraft by industry and government agencies have been initiated. An example of this type of work is reported in reference 2, which was done for STOL transports. The turboprop in reference 2 showed a 38 percent savings in fuel compared to a turbofan. Other references on the subject are 3 to 6. In reference 6 the author estimates that the optimum turbofan has a bypass ratio of 10.4, an overall pressure ratio of 40, and a fan pressure ratio of 1.6 at a noise goal of FAR-36 minus 10 dB. It is also estimated that the optimum turbofan used 22 percent less fuel than a current high bypass turbofan if it were installed on the same type of aircraft. Some of the references listed differ in results and conclusions, but all testify to the search for ways to save fuel. Many were written before the cost of fuel started to increase so rapidly in late 1973 and the full impact of present day fuel cost was not factored into their conclusions.

There are several ways to reduce commercial airline use of fuel. Flying slower reduces fuel consumption as does restricting flight frequency which forces load factors up. Improvements are possible to existing engines and aircraft that would reduce fuel consumption. Finally, an entirely new aircraft, engine, or both could possibly result in fuel savings. The purpose of this study is to investigate the fuel saving potential of regenerative turbofans on an advanced subsonic transport compared to an advanced turbofan and the same aircraft.

Regenerative turbofans are of interest because of their ability to absorb wasted thermal energy in the primary exhaust stream and use this energy to increase the air temperature entering the combustor. This in turn means that less fuel is needed to reach any given level of turbine-inlet temperature.

The regenerative turbofans in this study had a design-turbine-inlet temperature of 1700 K (3060° R). The overall pressure ratio was varied from 10 to 20, the bypass ratio from 8 to 10, the heat exchanger effectiveness from 0.80 to 0.90 and the heat exchanger pressure drop from 4 to 8 percent. The fan pressure ratio was fixed at 1.6 and the pressure drop in the ducts leading to and from the heat exchanger was fixed at 4 percent total. The heat exchanger itself was a ceramic matrix drum type that was mounted at the end of the last turbine stage on the engine centerline. This kept engine frontal area to a minimum but did lengthen the engine which resulted in some drag increases. All the engines were designed to operate at 10.67 kilometers (35 000 ft) and Mach 0.80. The design range was 5500 kilometers (3000 n mi) with a payload of 18 144 kilograms (40 000 lb) which is 200 passengers. As the aircraft changed design weight, the engines, wings, and landing gear were resized. The wing loading was held fixed at 5980 newtons per square meter (125 lb/ft²). Changes in engine and wing size resulted in drag changes to the aircraft.

SYMBOLS

ALPH heat transfer area/volume, m⁻¹

AR	aspect ratio
BPR	bypass ratio
Camber	camber of airfoil
C_{l0}	lift coefficient at minimum drag
C_{d0}	minimum drag coefficient
COND _M	conductivity of matrix material, W/m/K
c_p	specific heat at constant pressure, J/kg/K
CPR	compressor pressure ratio
D_{matrix}	diameter of matrix drum, m
D_{ref}	diameter of reference matrix drum, m
DH	hydraulic diameter of holes in matrix, m
FPR	fan pressure ratio
f/a	fuel to air ratio
HAR	ratio of cold to hot areas in the heat exchanger
IOC	indirect operating cost
L/D	lift to drag ratio of the aircraft
L_{matrix}	length of matrix drum, m
L_{ref}	length of reference matrix drum, m
CEW	operating empty weight of the aircraft
OPR	overall pressure ratio of the engine
ΔP_d	total pressure drop in all ducts leading to and from the heat exchanger
ΔP_h	total pressure drop across hot side of heat exchanger
ΔP_t	total pressure drop across hot and cold side of heat exchanger
RHOM	density of matrix material, kg/m ³
RTF	regenerative turbofan

SFC	specific fuel consumption, kg/hr/N
SIG	free flow area of matrix/frontal area
STOL	short takeoff and landing aircraft
T_4	turbine-rotor-inlet temperature, K
Tc-in	cold side air temperature into heat exchanger, K
Tc-out	cold side air temperature out of heat exchanger, K
TF	turbofan
Th-in	hot side gas temperature into heat exchanger, K
Th-out	hot side gas temperature out of heat exchanger, K
TOGW	takeoff gross weight, kg
t/c	thickness to chord ratio of the wing
W_c	compressor exit airflow, kg/sec
ϵ	effectiveness of the rotary heat exchanger

METHOD OF ANALYSIS

Mission

The mission assumptions were as shown in figure 1. Taxi-out was 9 minutes at idle power and takeoff was 1 minute at full power. The climb, cruise, and letdown accounted for the total range of 5500 kilometers (3000 n mi). Taxi-in was 5 minutes at idle power. The reserves consisted of 1 hour at the final cruise fuel rate, 2 minutes at full power for missed approach, and a 370 kilometer (200 n mi) alternate mission at lower speed and altitude. The normal cruise speed of the aircraft was Mach 0.80 at 10.67 kilometers (35 000 ft). The payload was assumed to be 18 144 kilograms (40 000 lb) or 200 passengers and baggage.

Aircraft

Aircraft layouts - Figure 2 is a sketch of the reference aircraft showing the general layout and engine placement. The sketch is meant to be representative of the family of advanced aircraft studied and not a precise drawing. In the case of the regenerative turbofan (RTF) the aircraft would look almost the same except the engines would definitely be longer and probably a little wider. Since the payload remained constant for all the aircraft studied, the fuselage also remained fixed. Only the

wing, landing gear, and engines changed. The wing changed size so that wing loading remained fixed at 5980 newtons per square meter (125 lb/ft^2) as takeoff gross weight (TOGW) varied.

Aircraft drag. - The assumptions that went into calculating the drag of the aircraft are shown in table I. These characteristics are typical for the type of aircraft studied in this report. Figure 3 shows the drag polar for the reference turbofan powered four-engine transport. The reference aircraft had engines with a bypass ratio BPR of 10.4 and an overall pressure ratio (OPR) of 40. The polar was generated by the aircraft mission analysis code (AMAC) which is an undocumented in-house code that calculates the airplane size, component weights, drag, mission fuel, and the direct and indirect operating cost (DOC and IOC). When engine types were switched, the drag of the reference TF engines was subtracted and the drag of the new engines was added as if they were isolated engines. The aircraft as designed achieves lift to drag (L/D) ratios that range from a little over 16 at the start of cruise to a little less than 15 at the end of the constant altitude cruise.

Engines

Reference turbofan. - A sketch of a typical turbofan engine is shown in figure 4(a). This engine was chosen because of its optimum fuel burning characteristics as discussed in reference 6. This engine also met the noise goal of Federal Air Regulation, Part 36 (FAR-36) minus 10 EPNdB. The cycle assumptions that went into the reference TF are shown in table II. The level of technology used in all the engines could be available early in the 1980's. All of the cycle calculations for the reference TF and the RTF were done using engine matching codes, references 7 and 8 or modified versions thereof.

Regenerative turbofan. - A sketch of a typical regenerative turbofan engine is shown in figure 4(b). The technology level of the engine itself, excluding the heat exchanger, was chosen to be of the same level as the reference TF engine. Cycle thermodynamic considerations require that the OPR be lower when a heat exchanger is used in this cycle. This is reflected in the values studied as shown in table II for the RTF. The sketch in figure 4(b) indicates the placement of the rotary drum matrix behind the low pressure turbine. It also indicates that while the compressor and low pressure turbine will most likely be reduced in stages and therefore length, the added length of the heat exchanger will most likely more than offset this. Thus the RTF will be somewhat longer than the reference TF. The diameter of the nacelle may also be increased due to the heat exchanger ducting which must pass around the case of the low pressure turbine thus forcing the bypass duct outward to some extent. The reverse flow combustors and radial compressor are other ways that could be used to shorten the RTF engine. The engine length calculation assumes they are used but an in depth design study would be needed to determine their final feasibility.

As noted in table II, the T_4 of the RTF is 1700 K while the T_4 of the reference TF is only 1615 K. Normally in a study of this type the T_4 of the competing cycles might be expected to be the same. The reference TF's T_4 was optimized in reference 6. That is why the 1615 K was used for that cycle. However, the RTF is a completely different cycle and changes in T_4 affect it differently. It will be shown later that the slightly higher T_4 of the RTF was necessary to minimize the fuel used. This was a result of the heat exchanger getting smaller as T_4 increased, which in turn helped reduce the drag and weight of the RTF engines.

Turbine cooling bleed. - The turbine bleed calculations are based on the full-coverage film technique described in reference 9. The reference TF assumed a one-stage high-pressure turbine and a four-stage low-pressure turbine. This resulted in a total chargeable cooling bleed flow of 8 percent as shown in table II. This bleed flow was taken from the exit of the high pressure compressor where the air is unusually hot due to the high OPR. It was estimated in reference 6 that if a heat exchanger was used between the cooling air and the fan bypass air, the resulting temperature of the turbine cooling air would allow the bleed flow to be reduced from 8 to 4.2 percent which in turn reduced the SFC by 2.8 percent. This lower SFC engine is not used as the reference TF in this report but is mentioned because the RTF engines did require such a heat exchanger for the cooling bleed in order to be competitive. This effect will be considered in the report at a later point.

The RTF engines in the report required the cooling bleed heat exchanger because with the higher T_4 's and the lower CPR's, the low pressure turbine encountered very high gas temperatures. As a result of this, the cooling bleed for the low pressure turbine was becoming very large and masking the otherwise good effect of the high T_4 on the RTF. The heat exchanger for the cooling bleed was assumed to have an ϵ of 0.85. No weight penalty was charged for the heat exchanger in this study. The effect of this assumption will be assessed later in this report.

Heat Exchanger

Design philosophy. - The heat exchanger in this study is a rotary regenerator. The rotating component is alternately exposed to the hot gas stream and the cold air stream. Thus, heat is at first absorbed and then given up by the matrix material. While disk-shaped regenerators are used in auto, truck, and power station applications, such a shape would pose a problem for a turbofan engine. The disk tends to have a very large diameter compared to the turbine case at the exit of the low-pressure turbine. Therefore, the packaging for an aircraft application would require putting the disk in a wing if the engines were wing mounted or in the fuselage if that is where the engines were mounted. In this study the engines were on the wing and the wing weight equations did not account for the disk structure. In this study the heat exchanger was assumed to be attached to the engine behind the low-pressure turbine on the

engine centerline. This arrangement was easier to analyze than the disk concept and appeared to minimize the heavy duct weights.

For this study the rotating matrix has been assumed to be a hollow ceramic drum. It would resemble a tin can with both ends removed. It was sized to fit behind the turbine case of every engine examined. The length and thickness are determined by the characteristics assigned to it at the design point. The greater the pressure drop allowed, the thicker the walls of the drum are and the shorter the drum becomes. The smaller the pressure drop allowed, the thinner the walls are and the longer the drum. A sketch of what the drum might look like behind an engine is shown in figure 4(b). The drum is of constant radius and the nozzle exit flows of the primary and secondary streams are shown in a way that could result in some mixing of the streams. The effect of mixing was not considered in the study due to the large uncertainties in the nozzle requirements and design at this preliminary stage. However, the velocity ratio between the primary and secondary stream was about 1.5 which is favorable for mixing.

Depending on the compressor pressure ratio chosen, it is likely that the compressor could be as much as 30 percent shorter than the compressor on the reference TF. It is possible that at least the final stage of compression might be supplied by a radial stage since the flow must be turned outward for ducting to the heat exchanger anyway. This would shorten the compressor even further. A detailed analysis beyond the scope of this report would be needed to determine the feasibility of such a scheme. The conditions entering the low pressure turbine determine the number of stages needed there. In some cases this means a reduction of stages there also compared to the reference TF. It is even possible that a reverse flow combustor might be practical since the airflow returning from the heat exchanger is traveling in a reverse direction around the outside of the turbine case already. So there are some tendencies for the RTF to have a shorter basic engine than the reference TF. This helps to offset, to some extent, the added length of the regenerator. Even with these differences, it is predicted that the RTF nacelle will be somewhat longer and slightly larger in diameter than the reference TF. The sketches in figure 4 try to show this.

More detailed sketches of a typical heat exchanger and the necessary duct work are shown in figures 5 and 6. It can be seen from these sketches that the cold air (compressor exit) enters two outer ducts opposite each other. These ducts are tapered to a reduced height at the rear of the matrix. By this time most of the flow has passed radially inward through the rotating matrix drum, has been collected in the inner ducts, and is flowing in a reverse direction toward the combustor (not shown). The hot turbine exhaust gas enters the two inner ducts and passes radially outward through the rotating matrix. It is collected in outer ducts and leaves in an axial direction producing thrust. Since the two flows are in opposite directions through the matrix, there is a natural tendency for the matrix to be self-cleaning.

The position of the seals is shown in figure 6. Since they are of some substantial length, it was found that they need back support for their entire length, in order to minimize leakage from the high to low pressure side. In the initial cycle calculation it was assumed that the leakage and carryover was zero. In the final results the effect of leakage and carryover was considered.

Theory. - The general theory and methodology used for the heat exchanger calculations was taken from reference 10. The actual subroutine used to calculate the size and weight of the matrix material was written by Mr. Paul Kerwin of the NASA Lewis Research Center. The heat exchanger effectiveness was an input at the design point and was defined as

$$\epsilon = \frac{T_{c_{out}} - T_{c_{in}}}{T_{h_{in}} - T_{c_{in}}} \quad (1)$$

Other inputs were:

HAR	0.25 to 1.0
ALPH.4602 m ⁻¹ (1402 ft ⁻¹)
DH	0.000634 m (0.00208 ft)
SIG	0.729
RHOM.	705 kg/m ³ (44 lb/ft ³)
CONDM	1.902 W/m/K (1.1 Btu/ft/hr/°F)
ΔP _t	4 to 8 percent
ΔP _d	4 percent

The idea was to input ϵ and go through the cycle to calculate $T_{c_{in}}$ and $T_{h_{in}}$. These terms would allow the calculation of $T_{c_{out}}$ from equation (1). A heat balance such as

$$W_c \times (1 + \beta) \times c_p \times (T_{c_{out}} - T_{c_{in}}) = W_c \times \left(1 + \frac{f}{a}\right) \times c_p \times (T_{h_{in}} - T_{h_{out}}) \quad (2)$$

allowed the calculation of $T_{h_{out}}$. An iteration was necessary since f/a was changing. Since turbine cooling bleed (β) was being calculated, it was also changing in equation (2), thus requiring an additional iteration. An additional iteration was necessary on top of the rest because the heat exchanger calculation divided up the ΔP_t into a $\Delta P(\text{cold})$ and a $\Delta P(\text{hot})$. These in turn occasionally changed the cycle performance enough to require rebalancing of the heat transfer.

In order to calculate the turbine case diameter the turbine-exit Mach number was assumed to be 0.45 and the hub-to-tip radius ratio of the last low-pressure-turbine stage was assumed to be 0.60. These are the same values used in the reference TF. The thickness of the matrix drum walls was a function of the ΔP_t mainly. The matrix weight was a function of the volume of material needed, which was in turn a function of

the heat to be transferred. Knowing the volume, the thickness and the required diameter of the matrix, the length was calculated.

Off-design calculations were accomplished by varying ΔP_t to achieve the proper thickness and varying ϵ to achieve the proper volume of the matrix material. It was assumed that the regenerator was in full operation at all off-design conditions. No determination was made if this was the best situation under such conditions as takeoff. It is possible that at takeoff it may be desirable to bypass the regenerator to get more thrust.

Weight

Heat exchanger weight. - While the weight of the heat exchanger matrix is a straightforward calculation, the weight of the heat exchanger ducts, seals, drive assemblies, and supporting structure is not. Previous in-house studies (not reported) resulted in a preliminary design of a heat exchanger for this application. As a result of this design effort a good first order approximation of these other weights was obtained. In this study these weights were scaled to account for different cycle effects on the heat exchanger size. The total weight of the heat exchanger (Wt. Hx) was

$$Wt. Hx = Wt. matrix + A + B \times \frac{D}{D_{ref}} \times \frac{L}{L_{ref}} \quad (3)$$

where

A was the weight of the ducts from the compressor to the heat exchanger and from there back to the combustor for the in-house designed RTF. 163 kg (360 lb)

B was the weight of the rest of the ducts in and around the heat exchanger plus the seals and the drive motors and supporting structures. 381 kg (840 lb)

D_{ref} 1.12 m (44 in.)

L_{ref} 1.78 m (70 in.)

Engine weight. - The bare engine weights were calculated by the method of reference 11. The nacelle and pylon weights are calculated for each of the engines assuming they are long duct engines. The other inputs necessary for the engine weight calculation are the airflow, BPR, OPR, T_4 , year of initial entry into service (1985), and the design Mach number. In the case of the RTF's, the weight of the heat exchanger must be added to the bare engine weight to get the total.

Aircraft weight. - The rest of the aircraft weights are calculated

by the AMAC program. Since the aircraft in this study had a fixed payload, 200 passengers, the fuselage remained fixed. As the engine size and weight changed the wing and landing gear changed. A weight breakdown by components is shown in table III for the reference turbofan-powered aircraft.

Cost

The cost of the airframe is a function of many things. Two of the main parameters are the quantity to be produced and the airframe weight. Since all the aircraft in this report will be treated equally, the absolute number to be produced has only a second order effect on a comparison. The assumed cost of the airframe per pound is shown in figure 7. It was taken from the center of the band of data reported in reference 12.

The cost of the turbofan bare engine (C_{eng}) and the cost of the RTF bare engine (without the heat exchanger) was estimated to be

$$C_{eng} \text{ in (1974 dollars)} = 1.2 \times 10^6 (\text{engine airflow}/1300)^{0.35} \quad (4)$$

The cost of the heat exchanger must be added to this in the case of the RTF engine. However, for the arrangement anticipated in the present application, no heat exchanger cost reference was found. So it was assumed to cost \$500 per pound, which is about what the turbofan engines cost per pound. The cost of the RTF engine was varied to determine the effect of direct operating cost (DOC).

Direct Operating Cost

No matter what method is used for calculating DOC, the absolute level is always in question. In this study, the aircraft being compared are essentially the same except for the propulsion differences. For this reason the percent change in DOC was used to make the comparisons. The 1967 ATA DOC method, reference 13, was used in this study. However, the equations were updated to 1974 dollars. Also, the engine maintenance formulas were not used. In their place the maintenance formulas developed by American Airlines were used (ref. 14). The cost of fuel was set at \$66.05 per cubic meter (25¢/gal) for this domestic range aircraft. This value corresponds to the average domestic price paid by United States airlines in December of 1974 according to the Civil Aeronautics Board (CAB). Fuel cost was varied from that level up to \$132.1 per cubic meter (50¢/gal) to determine its effect on the DOC comparisons.

RESULTS AND DISCUSSION

General Trends

Fuel against changes in SFC and propulsion system weight. - In a

study of this type it is important to use simple methods to determine the best cycle parameters to investigate in more depth. This is because the number of variables to be considered in the engine and heat exchanger are so numerous that the possible combination becomes too large to handle efficiently unless a prescreening of some sort is done. So, one of the first curves generated for this study shows the change in fuel used as SFC and propulsion system weight are varied (fig. 8). On this curve, a quick evaluation can be made for any propulsion system if the SFC and weight are known. For example: if a propulsion system weighed 4000 kilograms more than the reference system but provided a 10 percent reduction in SFC, the fuel saved would be 1270 kilograms. No account is made in this figure for changes in drag. That is a second order effect and will be evaluated after the initial screening.

Cycle, engine, and heat exchanger trends. - Figure 9 along with figures 11 and 12 use a relative scale to show the figure of merit trends. This is because the data was run under slightly different ground rules than the final data. So to avoid confusing comparisons of absolute values, these absolute values are omitted in these figures. This in no way appreciably changes the trends shown in these figures.

Some important trends that helped determine the impact of OPR and T_4 on the more important engine parameters are shown in figure 9. In part (a) of the figure it can be seen that increasing T_4 increases SFC. This is due in part to the low OPR's, the nonoptimum BPR, and the fact that more cooling bleed was needed for the turbines as T_4 was increased even though a precooler is assumed to precool the turbine cooling air with the duct stream air. Increasing OPR reduces SFC at any given T_4 . If the curves went far enough, there would be a minimum of course. The circular point on figure 9(a) is just a particular point which is common to figures 9, 11, and 12 and is therefore used as a reference point for the relative scale.

Part (b) of the figure shows that increasing T_4 does improve the thrust of the engine and thus reduce its size. Increasing the OPR has the same effect. So in both parts of the figure increasing OPR was good while increasing T_4 was good for thrust but bad for SFC.

Since the heat exchanger is a drum shape that fits behind the low pressure turbine, its length is important. A long heat exchanger will increase the nacelle length and therefore cause a weight and drag penalty. From figure 9(c) it is obvious that increasing T_4 reduces the heat exchanger length as does increasing the OPR. It would appear, therefore, that increasing T_4 and OPR to some point are both beneficial in reducing the heat exchanger length.

From figure 9(d) it can be seen that increasing T_4 and OPR are also beneficial in reducing the engine weight. Thus, the four parameters examined: SFC, thrust, heat exchanger length, and engine weight are all improved as OPR is increased to some point and three of the four improve as T_4 is increased.

One additional parameter that proved to be significant in reducing the heat exchanger size and weight was HAR (ratio of cold to hot areas). These trends are displayed in figure 10. This figure is for one engine only and neglects the fact that as HAR changes, the turbine case radius changes slightly. The effect of this will be discussed shortly.

The first part of the figure shows that as HAR is increased, well over 90 percent of the total pressure drop is across the hot side of the heat exchanger. This is presented for informational purposes but is of interest because the value of HAR finally selected was 0.7 where 99 percent of the pressure is dropped across the hot side. Part (b) of the figure is of interest because it is important that the walls of the matrix do not get too thin. Something on the order of 2 inches should be satisfactory for structural considerations.

The real heart of this figure is parts (c) and (d). In part (c) it will be noted that if HAR should be chosen at a low value, the length of the drum would be very large and so the engine would be very large. Thus there would be a large drag penalty for the engine. As shown in part (d) of the figure, the longer drum would result in longer ducts which according to equation (3) in the METHOD OF ANALYSIS would result in heavy ducts. As shown in figure 10(d), decreasing the value of HAR from 0.7 to 0.1 would increase the length of the heat exchanger three times, the matrix weight three times, and the entire heat exchanger weight 2.5 times. In the actual engine calculations the diameter of the low pressure turbine changed slightly as HAR varied. This caused a minimum in heat exchanger weight and length to occur between HAR of 0.6 and 0.8. Since the curves were pretty flat in this region, the HAR value of 0.7 was chosen from that data and retained for the rest of this study.

Selecting the Range of Cycle Variables

From reference 6 the best advanced turbofan had a FPR of 1.6 at cruise and a T_4 of 1615 K. The FPR was selected at as high a value as could be tolerated by the FAR 36 - 10 dB noise criteria selected for that study. Since that is basically the reference turbofan used in this study, the FPR selected for the RTF was also 1.6. However, due to the nature of the regenerative turbofan, it was felt to be unfair to restrict the T_4 studied to 1615 K. This, after all, is one of the main controls used to size the heat exchanger. Thus it was felt that the value of T_4 should be picked based on its merits in the RTF.

In order to determine the best range and combination of cycle parameters, figure 11 can be examined. From the previous discussion of figure 9 it will be recalled that only the SFC got worse with increasing T_4 . So, with the aid of figure 10(a) it can be seen that the minimum SFC for a FPR of 1.6 occurs near a BPR of 8.0. This is at a T_4 of 1590 K. The entire figure 10(a) is for a ϵ of 0.80 and the turbine cooling air pre-cooler is assumed to be used in this figure and figure 12.

If the level of ϵ is increased to 0.90 as in figure 10(b), the minimum SFC still occurs around a BPR of 8.25 and a $T_4 = 1590$ K. So from SFC considerations alone, this might be a good area to investigate. It will be recalled from previous discussions that increasing T_4 did result in shorter, lighter, smaller engines. If this trend were to continue, a T_4 above 1590 K might be slightly better. So at this point it is not obvious that a T_4 of 1590 K represents the best trade between SFC and size and weight.

For these reasons figure 12 was constructed. This figure takes into account the weight effects of the propulsion systems. With the aid of figure 8 the effect of SFC and weight were combined to show the effect on fuel burned. The same range of T_4 was investigated over a range of OPR from 10 to 20. Note that the minimum fuel used in both cases occurred at or near a T_4 of 1700 K instead of 1590 K. So the suspicion that lighter engine weights might tip the scale in favor of T_4 's higher than 1590 K is borne out by the results shown in figure 12.

It was concluded from figures 9 to 12 that for this study a T_4 of 1700 K should be used in conjunction with the FPR of 1.6. It was further decided that the BPR should be varied from 8 to 10. Other in-house studies led to the conclusion that the ΔP_t for the heat exchanger should be varied from 4 to 8 percent, that the ϵ should be varied from 0.80 to 0.90, and that the OPR should be varied from 10 to 20. Thus the range of parameters studied is shown below.

FPR	1.6
OPR	10, 15, 20
T_4	1700 K
ϵ	0.80, 0.85, 0.90
ΔP_t	4, 6, 8 percent

This results in 81 engine combinations which are still too many to investigate in real depth. So, some further sorting had to be done.

General Results Excluding Drag, Leakage, and Carryover Effects

The next five figures will describe how the nine best engines were selected from the 81 engine matrix and the results of the fuel use calculations for these nine engines. At this point the calculations are still done using figure 8. This means that the drag effect of different length engines is not considered at this point. Also the effect of seal leakage and carryover losses is not included in any of the performance values at this point. The effect of these parameters will be considered later.

Figure 13 is for an $\epsilon = 0.80$ and a $\Delta P_t = 4$ percent. It covers nine engine combinations of OPR = 10, 15, and 20 and BPR's of 8, 9, and 10. The trends in SFC shown in figure 13(a) indicate SFC is improving as BPR increases. However, the minimum point is at increasingly higher OPR as BPR increases. The lower thrust per pound of air that goes with the

higher BPR's means a larger engine. Thus in figure 13(b) it turns out the lightest engines are at a BPR of 8. Combining the effects of weight and SFC by using figure 8, the fuel change can be plotted for these nine engines in figure 13(c). The best BPR depends on the OPR. At an OPR of 10, the best BPR is 9 but at OPR's greater than 15, the best BPR is 10. What is shown in the figure as a dashed line is a minimum envelope curve which indicates that the very best engine would have an OPR of 17 and a BPR of 10. So out of these nine engines, that one was chosen as best.

The next nine engines cover the same range of parameters but the ϵ is 0.85 instead of 0.80. This data is shown in figure 14. Note that the improvement in SFC is greater than in figure 13 due to the higher ϵ . The higher ϵ also means a larger heat exchanger and less thrust per pound of air which drives the engine weight up some compared to figure 13. When the changes in SFC were combined with the weight changes, the fuel changes could be plotted in figure 14(c). Note that due to the higher ϵ , the optimum OPR has been reduced from 17 in figure 13 to 14 in figure 14(c). The optimum BPR is now 9.5.

In figure 15 can be seen exactly the same trends. This is for an ϵ of 0.90. The SFC is still improving, the weight is still increasing, and the fuel savings is still improving. The effect of drag on the larger engines is still not included in the calculations at this point as was mentioned earlier. This will be shown to minimize the benefits of increasing ϵ later. Note the optimum OPR is now 12 at a BPR of 9.25. This decreasing optimum OPR is due to the increasing level of ϵ . More of the temperature rise before the combustor is being accomplished by heat exchange; therefore, less is needed by compression.

So far, figures 13 to 15 have shown the trends as ϵ increased from 0.80 to 0.90. Figure 16 is meant to show the effect of P_t at a constant ϵ of 0.85. So figure 16 should be compared to figure 14. Notice that the trends are about the same in the two figures but due to the greater ΔP_t in figure 16, the SFC benefits are not as great. The greater ΔP_t does, however, reduce the heat exchanger length and thus its weight. The engine weight shown in figure 16 is less therefore than in figure 14. This lower weight is not enough to offset the degraded SFC however, and thus the fuel saved as shown in figure 16(c) is not as great as in figure 14(c). When the drag of the shorter engine is included later this trend will be shown to reverse. The optimum OPR in figure 16(c) is 15 at a BPR of 9.25. This is nearly the same as that for figure 13(c).

In each of the figures 13 to 16, nine engines were examined and one optimum determined for each nine. This process was completed even though all of the data are not presented here. Thus from the 81 engines examined, nine were selected for further analysis. These nine are listed by their cycle characteristics below.

ϵ	ΔP_t , percent	Optimum OPR	Optimum BPR
0.80	4	17	10.0
.85	↓	14	9.5
.90	↓	12	9.25
.80	6	17	10.0
.85	↓	15	9.5
.90	↓	13	9.25
.80	8	18	10.25
.85	↓	15	9.25
.90	↓	12	9

Figure 17 is meant to be a summary up to this point. The optimum OPR and BPR is plotted against ϵ for the three levels of ΔP_t . Thus all nine of the optimum engines are represented in each part of figure 17. The basic trends are toward lower OPR as ϵ is increased. This in return will support lower BPR's as shown in part (b) of the figure. The fuel saved shows a tendency to linearly increase with ϵ . At low levels of ϵ the lower levels of ΔP_t are best, but at the higher levels of ϵ , the higher levels of ΔP_t are starting to look better. The most fuel saved is about 1630 kilograms (3600 lb).

Result Including Drag

The nine best engines were actually flown in a flight deck (AMAC) which accounts for the drag of different size engines. The results are shown in figure 18. Note that in figure 18(a) the curves have a minimum in contrast to figure 17(a). This is because the higher levels of ϵ require a longer heat exchanger and results in higher drag and heavier ducts. For the same reasons the greater ΔP_t now look better than the lower ΔP_t . Higher ΔP_t heat exchangers result in thicker walled drums which are in turn shorter and thus reduce the drag and duct weight. In terms of percentage, the best engine would appear to save about 5 percent in fuel compared to the reference TF. If higher ΔP_t were used, the envelope around those curves would bottom out at about 6 percent fuel saved.

The TOGW reduction at this point is about 1 percent or a little more according to figure 18(b). The gain here is less because of the heavier engines offsetting some of the SFC benefits.

The DOC change is plotted in figure 18(c). All of the changes are positive. This is due to the cost of the RTF engines which includes the cost of the heat exchanger. This area of heat exchanger cost is relatively unknown and thus the cost of the engine will be varied parametrically to show what the cost would have to be in order to break even. This will be done in a following figure. First however, the effects of

leakage and carryover are considered.

Results Including Carryover and Leakage

Sensitivity studies were performed that showed for every 1 percent of leakage or carryover loss, the SFC suffered 0.6 percent. Furthermore, the designers estimated the leakage could be held to 2 percent and the carryover to 1 percent for a total 3 percent. Thus the SFC would be degraded by 1.8 percent. Since small changes in SFC result in about the same change in fuel, about 1.8 percent of the fuel saved should be subtracted from the curves in figure 18(a). When this is done, figure 19 is the result. In figure 19, the curves were cross plotted so the curves could be extrapolated to higher ΔP_t (the dashed lines). If an envelope were drawn around these curves, the most fuel would be saved at a ΔP_t of about 12 and an ϵ of 0.91. At this point about 4.1 percent of the fuel would be saved and the reduction in TOGW would be expected to still be near 1 percent.

As was mentioned in the "METHOD OF ANALYSIS," the reference TF did not use a precooler for the turbine cooling bleed but the RTF did. Therefore, the comparison could be questioned on this basis. If this difference is accounted for, the reference TF's SFC would improve 2.8 percent. This would translate almost directly into a 2.8 percent fuel savings if the weight penalty of the heat exchanger is ignored. Thus the 4.1 percent fuel advantage of the RTF shown in figure 19 would be eroded to 1.3 percent or in other words, the two concepts would be very competitive from the fuel standpoint. The weight of the extra heat exchanger was not considered because it would be nearly the same on either type of engine, thus, not affecting the comparison to any significant degree.

Because the time required to design the heat exchanger ducts for low pressure drop was too demanding, they were mainly designed for structural consideration. It was hoped that a refined design would result in ducts which had a minimum pressure drop. The number used in this report was 4 percent which represents a reasonably ambitious goal. It could be argued, however, that this pressure drop might be larger. In that case the RTF performance would be decreased from that shown in figure 19. To show the effect of the ΔP_d assumption, the effect of ΔP_d on fuel used is shown in figure 20. It can be seen from the figure that an increase in ΔP_d would cause an increase in SFC which would cause an increase in fuel used. For small changes in SFC, the changes in fuel would be about the same percent. So if the ΔP_d was 10 percent instead of 4 percent, the RTF would use about 2 percent more fuel thus reducing the gains shown in figure 19 by a like amount.

Table IV compares weights, costs, and DOC of the reference TF and the best RTF for which data was actually calculated. This would be an engine with a $\epsilon = 0.90$, $P_t = 8$ percent, FPR = 1.6, OPR = 12, BPR = 9, HAR = 0.70, and a $T_4 = 1700$ K. The best engine shown in figure 19 would be very similar but the ϵ would be 0.91 and the ΔP_t would be 12 per-

cent. The OPR and BPR would probably change some small amount toward a smaller number.

Effect of Engine and Fuel Price on DOC

The cost of the basic engine in front of the regenerator on the RTF was based on airflow of the fan, as was discussed in the "Method of Analysis." This may not be exactly right due to the low OPR of the gas generator and the other unusual features. The cost of the heat exchanger was also roughly estimated. Thus the actual cost of the RTF is more questionable than that of the reference TF where the engine is more conventional.

The cost of the RTF, compared to the reference TF, is explored in figure 21 as fuel price is allowed to vary. The seal and carryover losses are included for the RTF in this figure so the fuel savings is only 4.1 percent. When the RTF engine costs 1.65 times as much as the reference TF, the DOC will be 6.6 percent higher than the reference TF at a fuel price of \$66 per cubic meter (25¢/gal). Within the range of the fuel prices investigated, the DOC of the RTF would never be as low as that of the reference TF at this engine price ratio. The fuel savings of 4.1 percent is just not enough to offset the higher engine cost. When the engine cost of the RTF is only 1.25 times that of the reference TF, the DOC's will be the same at a fuel price of \$135 per cubic meter (51.5¢/gal).

Figure 21 indicates that the cost of the RTF would have to be nearly equal to the cost of the reference TF before appreciable benefits in DOC could result. This is reasonable since the TOGW is nearly equal and only 4.1 percent of the fuel was saved. So in the final analysis, the trade off here is between the maintenance problems of high pressure ratio TF's and those of a heat exchanger behind a relatively low pressure ratio TF. Which would be the hardest to maintain is not known at this time, nor is the cost of the RTF really clear. Some hardware developments and tests could go a long way to resolve these unknowns.

CONCLUSIONS

The fuel savings potential of a reference advanced turbofan was calculated and compared to that of a family of advanced regenerative turbofans for use in an advanced subsonic transport. The main figure of merit was fuel consumed. However, takeoff gross weight (TOGW) and direct operating cost (DOC) were also calculated. The reference turbofan had a cruise turbine-rotor-inlet temperature of 1615 K while the regenerative turbofans cruised at their optimum of 1700 K. The overall pressure ratio of the reference turbofan was 40 while the optimum for the regenerative engines ranged from 12 to 18. All the engines had a fan pressure ratio of 1.6 at a cruise speed of Mach 0.80 and 10.67 kilometers (35 000 ft). The bypass ratio of the reference turbofan was 10.4 while that of the regenerative

engines ranged from 8 to 10. The rotary heat exchanger used a ceramic matrix shaped as a hollow drum which fit behind the low pressure turbine on the engine centerline. The range of effectiveness investigated was 0.80 to 0.90 along with pressure drops from 4 to 8 percent in the matrix and 4 percent in the ducts. A leakage of 2 percent and a carryover of 1 percent was allowed. The aircraft carried 200 passengers, a total of 5500 kilometers (3000 n mi). The aircraft cruise L/D was about 16.

The study indicated a fuel savings by the best regenerative turbofan of 4.1 percent compared to the reference turbofan. The TOGW improvement was a modest 1 percent while the DOC ranged from competitive values to as much as 6 percent higher depending on the actual cost of the regenerative turbofan and the cost of the fuel. In order to use the high turbine-rotor-inlet temperatures in the regenerative turbofans, a turbine cooling air heat exchanger was needed to precool the cooling air. The heat exchanger was assumed to be in the fan bypass stream. If this same advantage was given to the reference turbofan, the regenerative turbofan would have saved only 0.5 percent of the fuel and the TOGW would have been nearly equal for the two concepts.

It is the conclusion of this report that for this application either a high pressure ratio turbofan or a low pressure ratio regenerative turbofan would use about the same amount of fuel and result in an aircraft of about equal TOGW. The deciding factors would be the engine costs, the reliability of the two competing concepts, their maintainability, and possibly the relative ease of meeting some emission standards. Since the RTF does use a low overall pressure ratio, the problem of emissions may be more easily solved. Not enough is known about either concept at this time to determine these factors.

REFERENCES

1. Aviation Forecasts Fiscal Years 1975-1986. Federal Aviation Administration, 1974.
2. Scherrer, Richard; Olsen, Robert. Design Comparison of Quiet M 0.80 STOL Transports. SAE 710759, Sept. 1971.
3. Maddalon, D. V.: Rating Aircraft on Energy. Astron. Aeron., vol. 12, no. 12, Dec. 1974, pp. 26-43.
4. Rosen, George: Prop-Fan - A High Thrust, Low Noise Propulsor. SAE Paper 710470, May 1971.
5. Kraft, G.; and Strack, W.: Preliminary Study of Advanced Turboprops for Low Energy Consumption. NASA TM X-71740, 1975.
6. Knip, G.: Preliminary Study of Advanced Turbofans for Low Energy Consumption. NASA TM X-71663, 1975.

7. Fishbach, Laurence H.; and Koenig, Robert W.: GEN 2: A Program for Calculating Design and Off-Design Performance of Two- and Three-Spool Turbofans with as Many as Three Nozzles. NASA TN D-6553, 1972.
8. Shapiro, S. R.; and Caddy, M. J.: NEPCOMP - The Navy Engine Performance Program. ASME Paper 74-GT-83, Mar. 1974.
9. Kraft, Gerald A.; and Whitlow, John B., Jr.: Optimization of Engines for a Commercial Mach 0.98 Transport Using Advanced Turbine Cooling Methods. NASA TM X-68031, 1972.
10. Kays, W. M.; and London, A. L.: Compact Heat Exchangers. 2nd Ed., McGraw-Hill Book Co., Inc., 1964.
11. Gerend, Robert P.; and Roundhill, John P.: Correlation of Gas Turbine Engine Weights and Dimensions. AIAA Paper 70-669, June 1970.
12. Analysis of Operational Requirements for Medium Density Air Transportation. (MDC-J4484, Douglas Aircraft Co.; NAS2-8135.) NASA CR-137604, 1975.
13. Standard Method of Estimating Comparative Direct Operating Costs of Turbine Powered Transport Airplanes. Air Transport Association of America, Dec. 1967.
14. Sallee, G. Phillip: Economic Effects of Propulsion System Technology on Existing and Future Transport Aircraft. (American Airlines, Inc.) NASA CR-134645, 1974.

TABLE I. - BASIC AIRCRAFT DRAG INPUT DATA

AR	9.4
t/c side of body	0.164
t/c wing tip	0.080
Leading edge sweep, deg	27.4
Taper (tip cord/root cord)	0.33
Camber	0.07
Wing loading, N/m ²	5980
C _{l0}	0.06
^a C _{d0}	0.022
Supercritical wing	Yes

^aCalculated value from AMAC Program.

TABLE II. - CYCLE INPUTS AT THE CRUISE DESIGN POINT

Engine type	Ref. TF	RTF
Inlet recovery	1.0	1.0
Overall pressure ratio	40	10 to 20
Fan pressure ratio	1.6	1.6
Cruise turbine rotor inlet temperature, K	1615	1700
Adiabatic efficiency of the		
Fan	0.86	0.86
Compressor	0.85	0.854 to 0.865
All turbines	0.90	0.90
Efficiency of the combustor	1.0	1.0
Turbine cooling bleed, percent of compressor air	8.0	7.0 to 8.5
Cooling bleed precool heat exchanger	No	Yes
Cv, both nozzles	0.98	0.98
Pressure loss, $\Delta P/P$:		
Fan duct	0.02	0.02
Combustor	0.06	0.06
Turbine exit guide vanes	0.012	0.012
Heat exchanger cold side	-----	<0.005
Heat exchanger hot side	-----	0.035 to 0.075
Total of heat exchanger ducts	-----	0.04
Area cold side/area hot side (heat exchanger)	-----	0.7 (opt)
Heat exchanger leakage, percent	-----	2
Heat exchanger carryover, percent	-----	1
Heat exchanger effectiveness	-----	0.8 to 0.9
Number of spools	2	2
Bypass ratio	10.4	8 to 10
Altitude, km	10.67	10.67
Mach number	0.80	0.80

TABLE III. - TYPICAL WEIGHT BREAKDOWN OF AIRCRAFT DESIGNED FOR
MACH 0.80 USING THE REFERENCE TURBOFAN ENGINES

Structure weight, kg	27 211	Operating items, kg	5 293
Wing	9 801	Flight crew (3)	231
Horizontal tail	1 353	Cabin crew (7)	413
Vertical tail	852	Crew baggage	113
Body	8 955	Briefcases and navigation	11
Landing gear	3 884	Unusable fuel	133
Nacelle struts	844	Oil	91
Nacelles	1 522	Emergency equipment	5
		Passenger accommodations	3 107
Propulsion system weights, kg	5 675	Cargo containers	1 207
Four engines	3 375	Operating empty weight, kg	52 736
Accessories	181	Usable fuel, kg	26 226
Noise suppression	408	Payload (200 passengers), kg	18 144
Controls	72	Cargo, kg	0
Starting system	91		
Fuel system	544		
Thrust reversers	1 004		
Fixed equipment weight, kg	14 557	Takeoff gross weight, kg	97 106
Instruments	313		
Surface controls	1 787		
Hydraulic system	510		
Pneumatic system	315		
Electrical system	986		
Electronics	597		
Flightdeck accommodations	410		
Passenger accommodations	6 790		
Cargo accommodations	1 056		
Emergency equipment	292		
Air conditioning	976		
Anti-icing	143		
Auxiliary power units	382		

TABLE IV. - COMPARISON OF ENGINE TYPES AT MACH 0.80
ON A 5500 KILOMETER (3000 N MI) MISSION

Engine type	Reference TF	RTF ^a
Weights, kg		
TOGW	97 106	96 243
OEW (less propulsion system)	47 061	46 949
Wing	9 801	9 724
Landing gear	3 884	3 849
Other	33 376	33 376
Propulsion system (less nacelles)	5 675	6 254
Four engines	5 675	3 943
Four rotary heat exchangers	-----	2 311
Payload (200 passengers)	18 144	18 144
Design point fuel load	26 226	24 896
Fuel used	21 145	20 062
Reserve fuel	5 081	4 834
Initial costs, 10 ⁶ \$ (1974)		
Complete aircraft	15.042	18.206
Aircraft (less engines)	9.673	9.654
Each complete engine	.921	1.533
Bare engine	.921	.896
Heat exchanger	-----	.637
Spares	1.685	2.420
Direct operating cost, ¢/seat/km		
DOC	0.525	0.556
Relative DOC	1.00	1.06

^aNo seal leakage or carryover loss included.

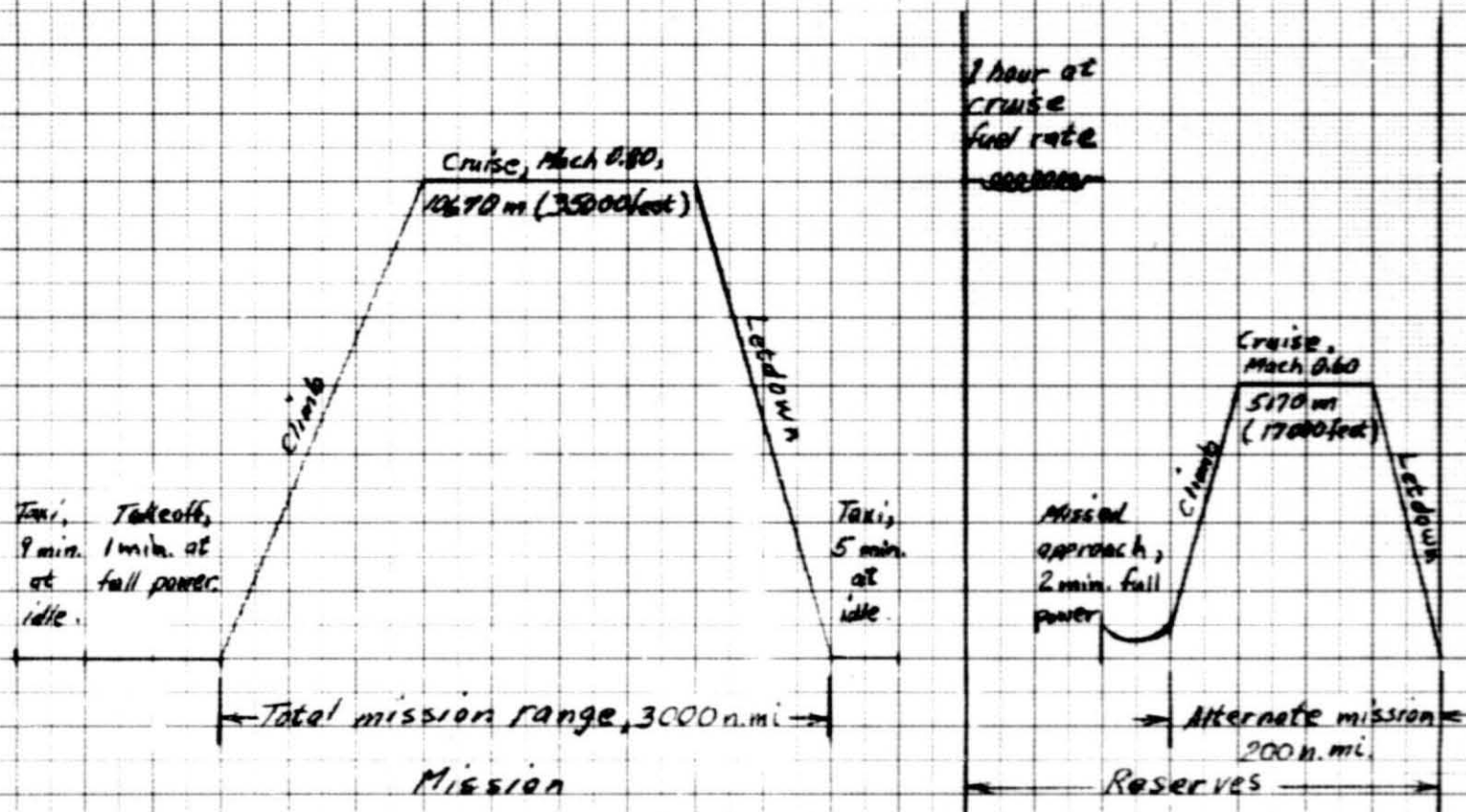


Figure 1.- Mission and reserve assumptions.

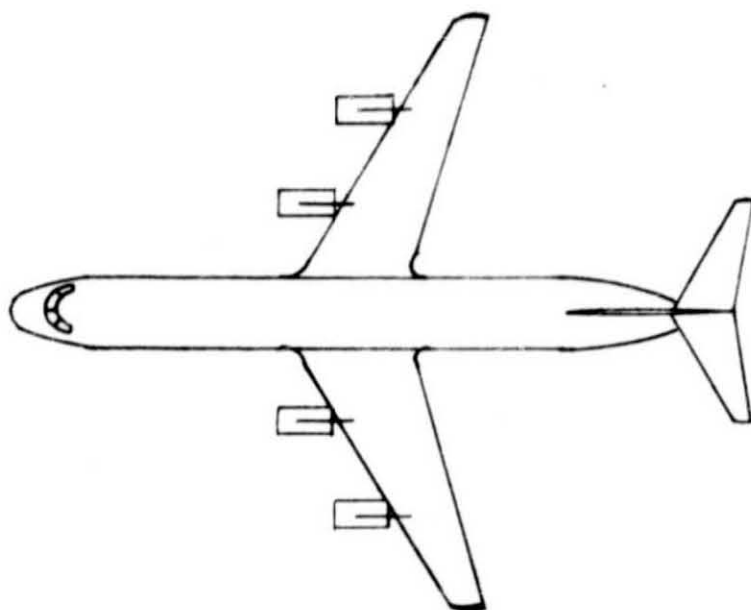
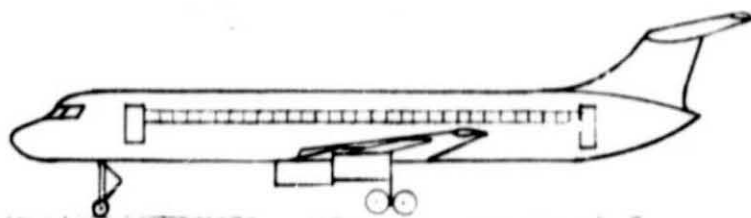


Figure 2.- Sketch of reference aircraft

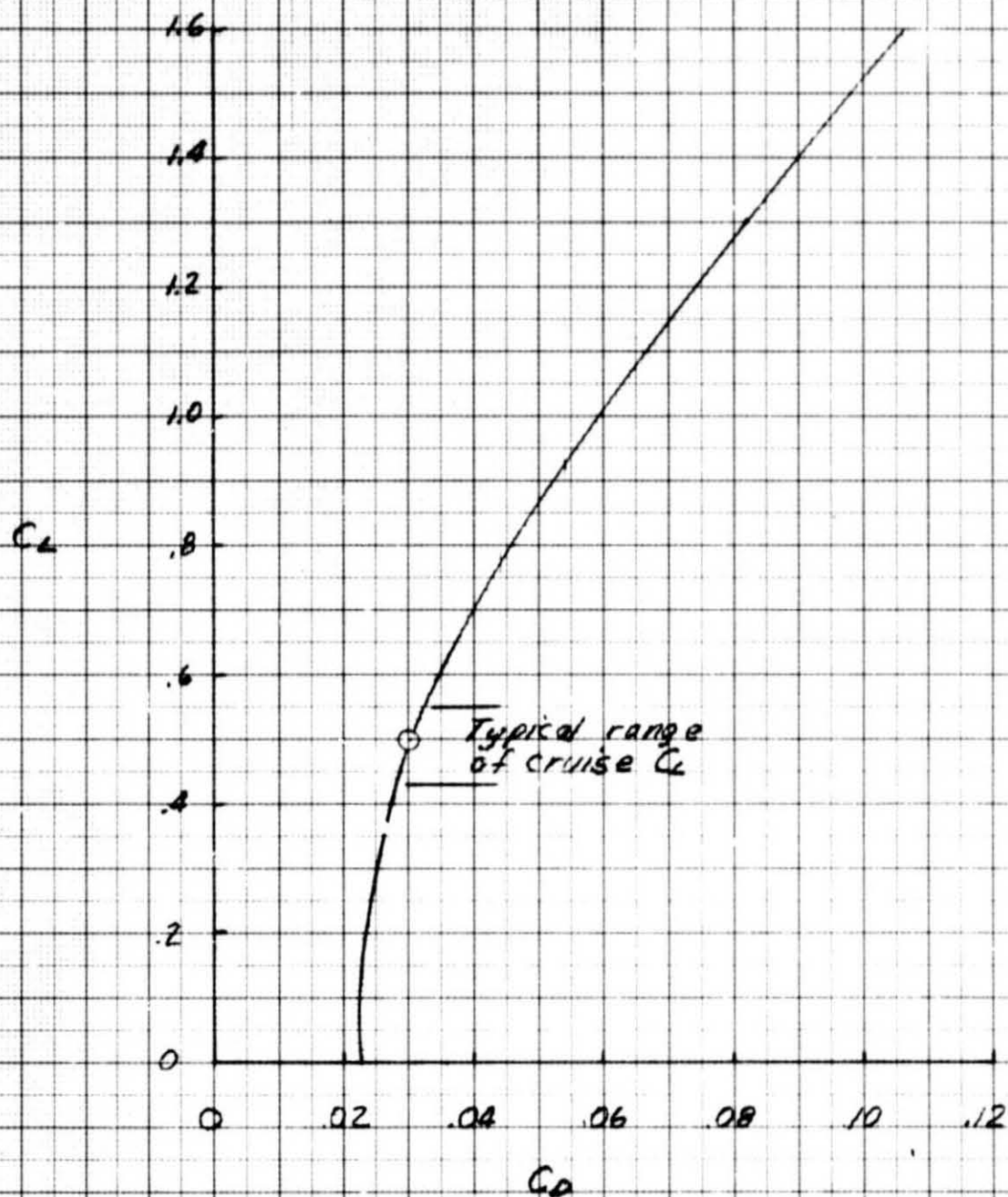
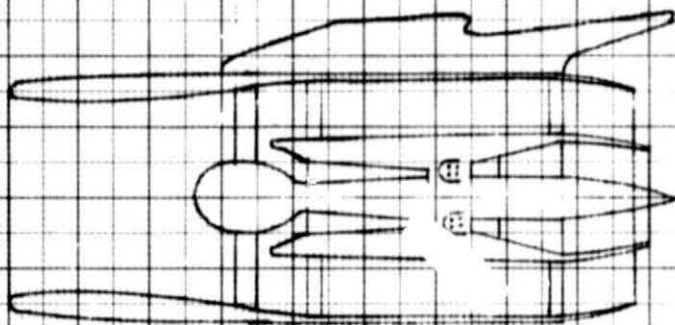
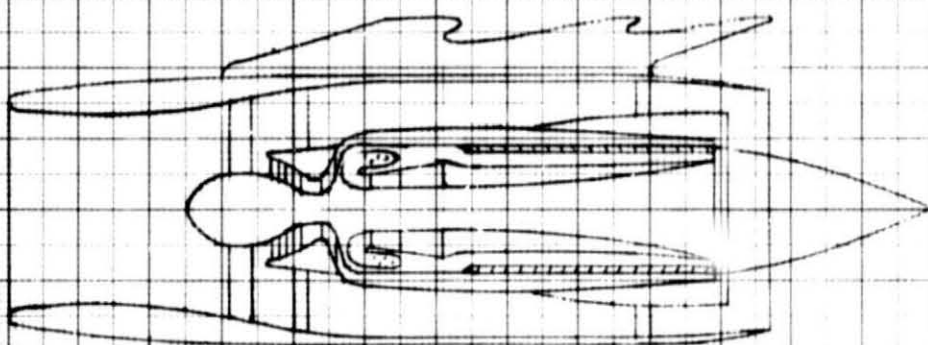


Figure 3. - Drag polar for 3000 n. mi. range aircraft, Mach 0.80 cruise.



a) Reference turbofan



b) Regenerative turbofan

Figure 4.- Sketch of typical high bypass ratio turbofan engine with and without regenerator. Relative size of nacelles and engine components is approximately correct.

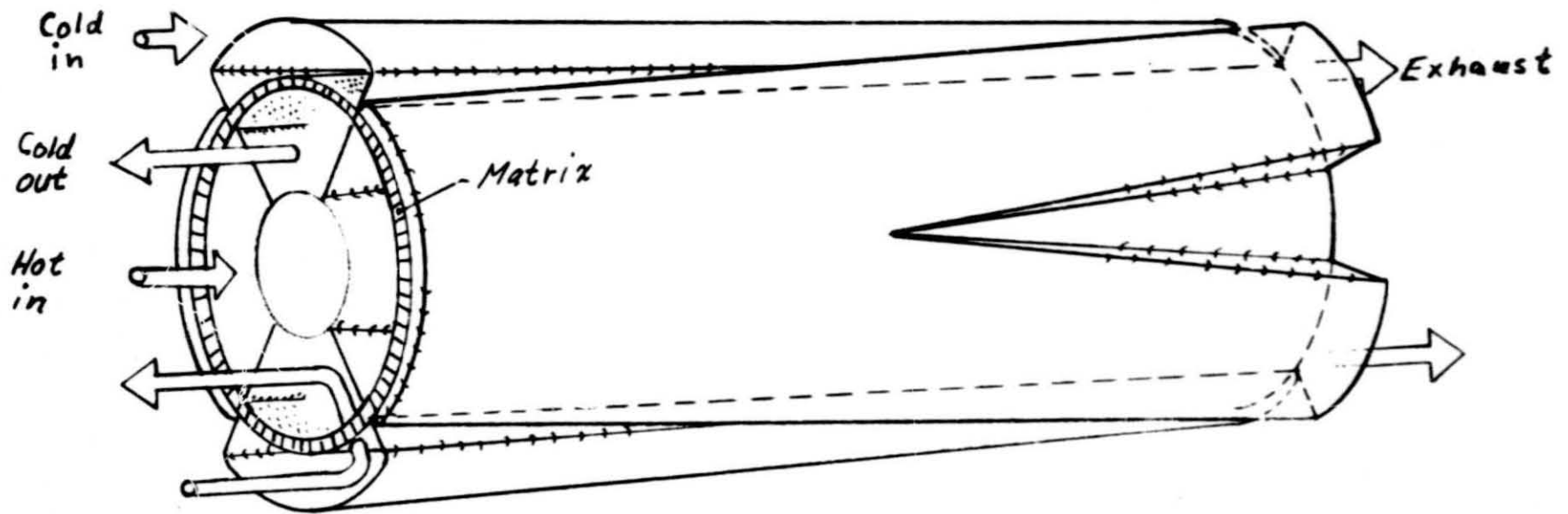


Figure 5.- Heat exchanger sketch, oblique view

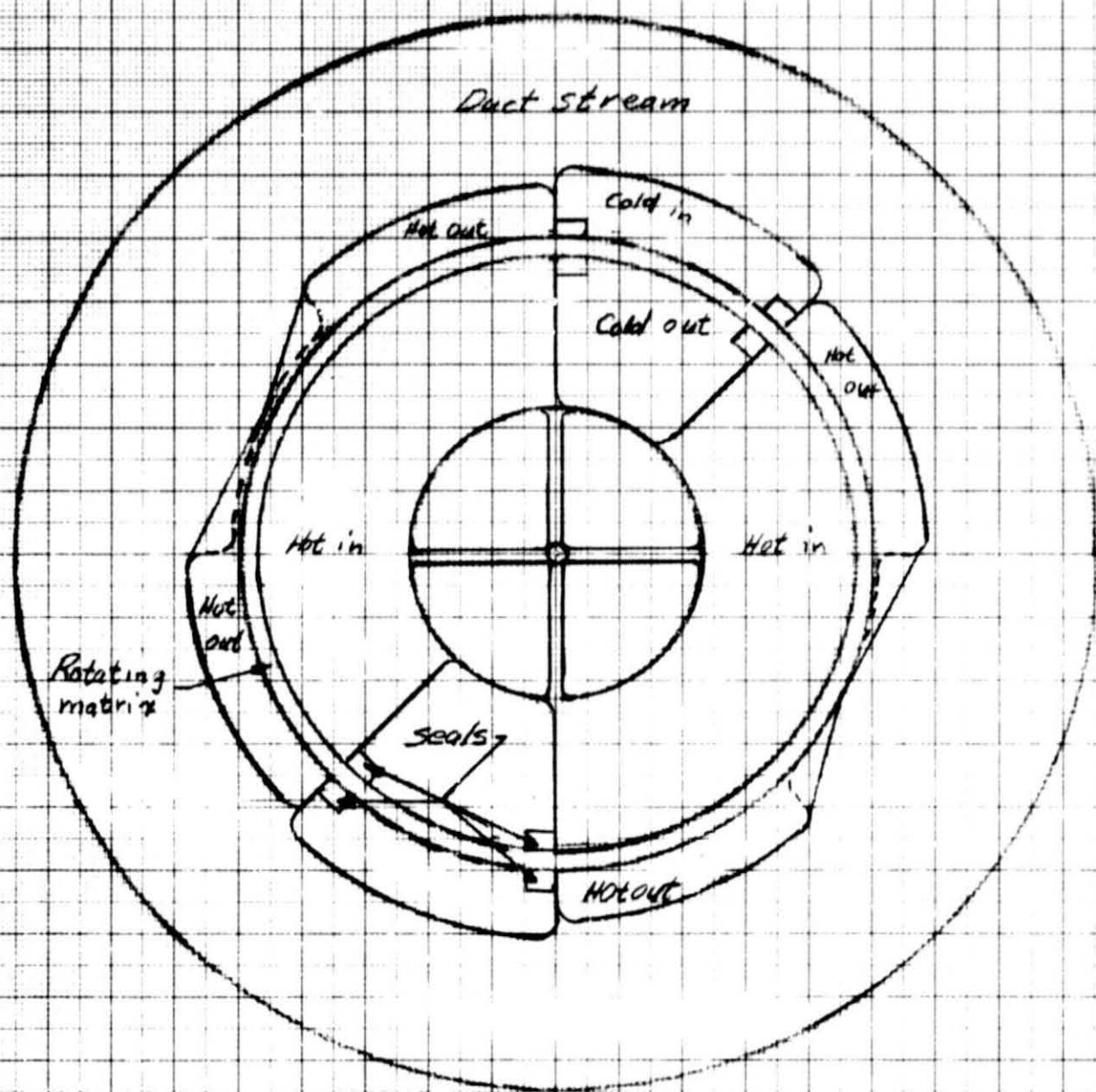


Figure 6 - Heat exchanger sketch, front view

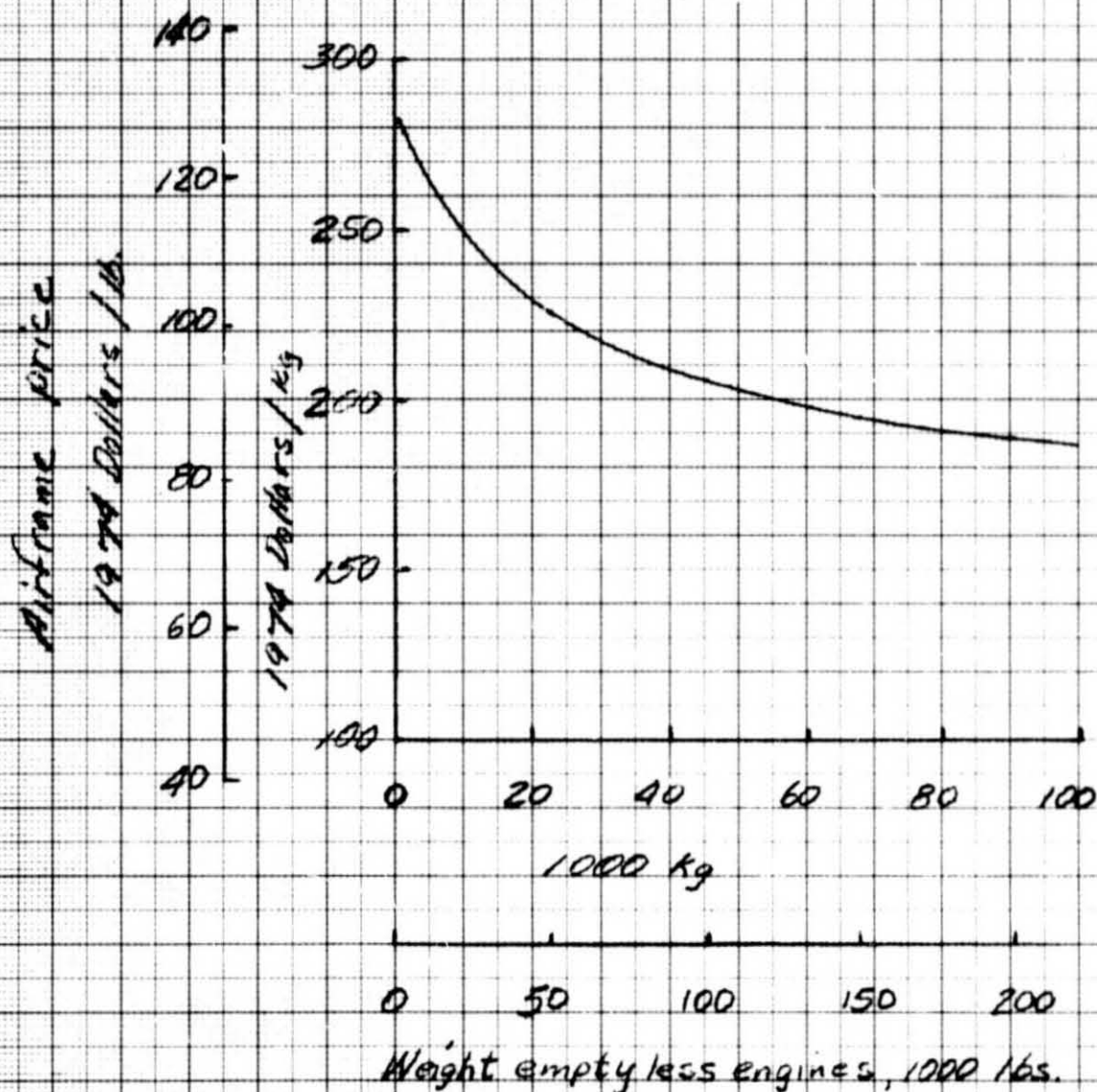


Figure 7 - Airframe price versus weight

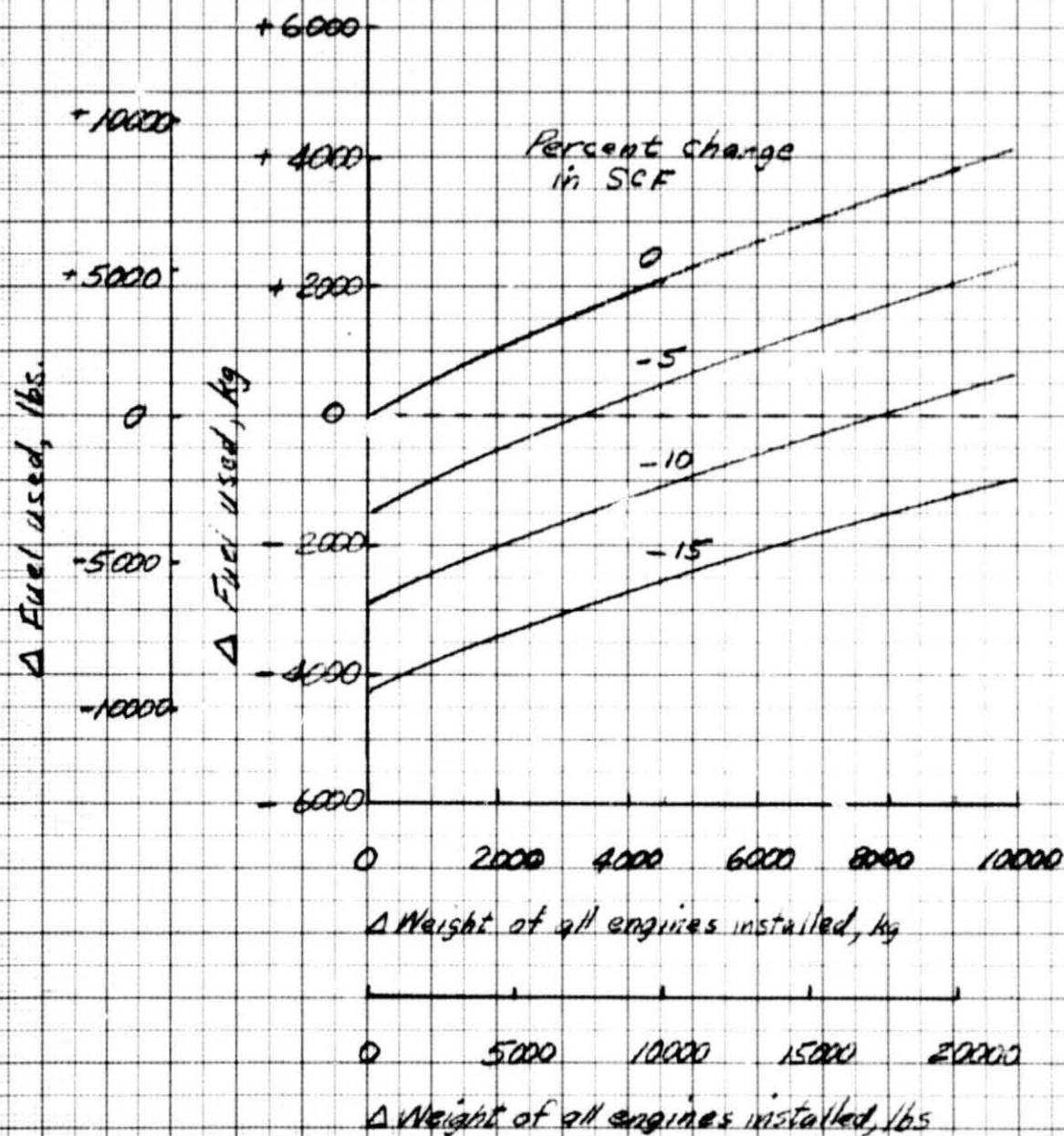


Figure. - 8 Change in fuel used per flight

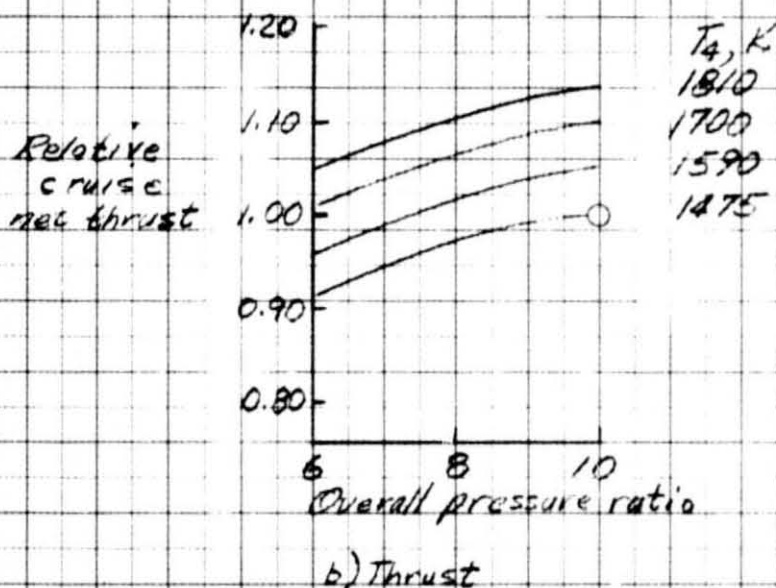
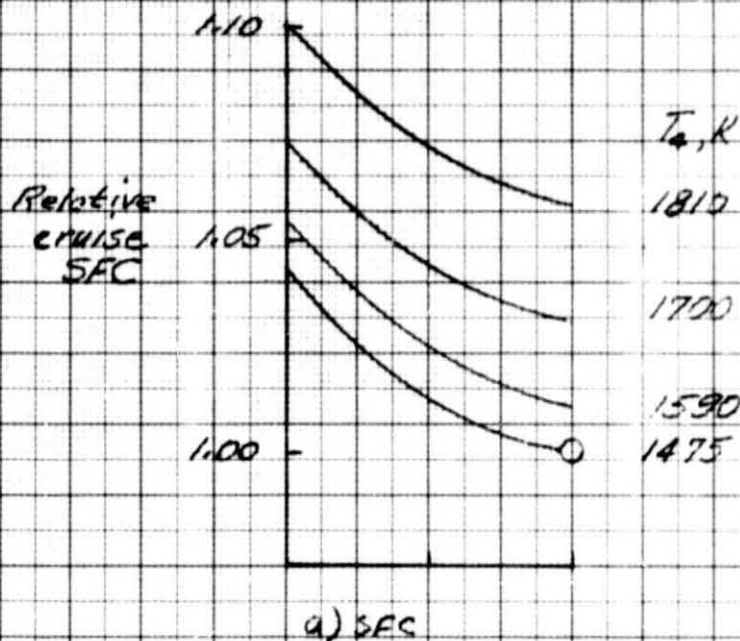
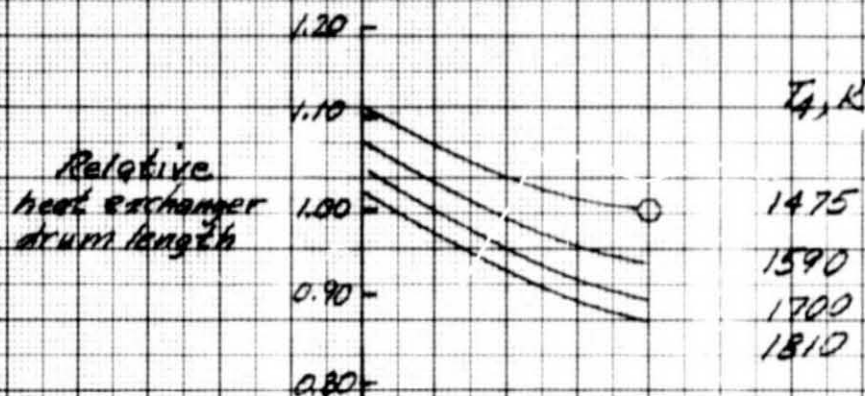
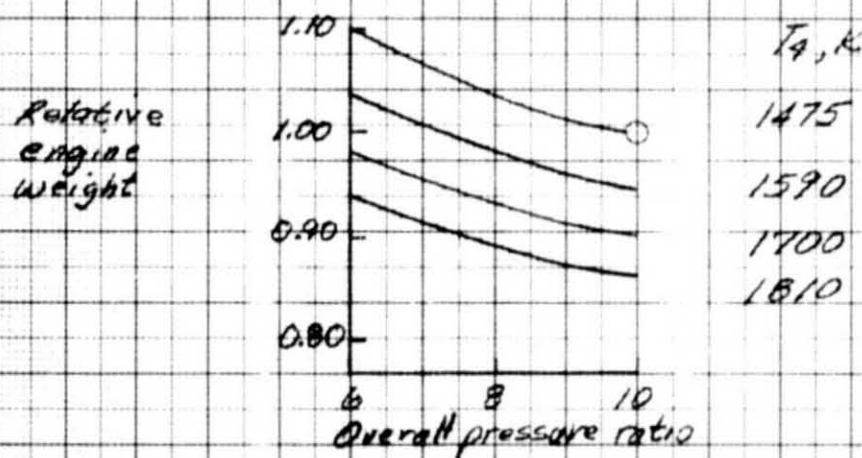


Figure 9. - The effect of OPR and turbine-rotor-inlet temperature on engine and heat exchanger parameters. Design FPR=2.0, BPR=4.5, $\epsilon=0.20$, $\Delta P_e=12\%$.

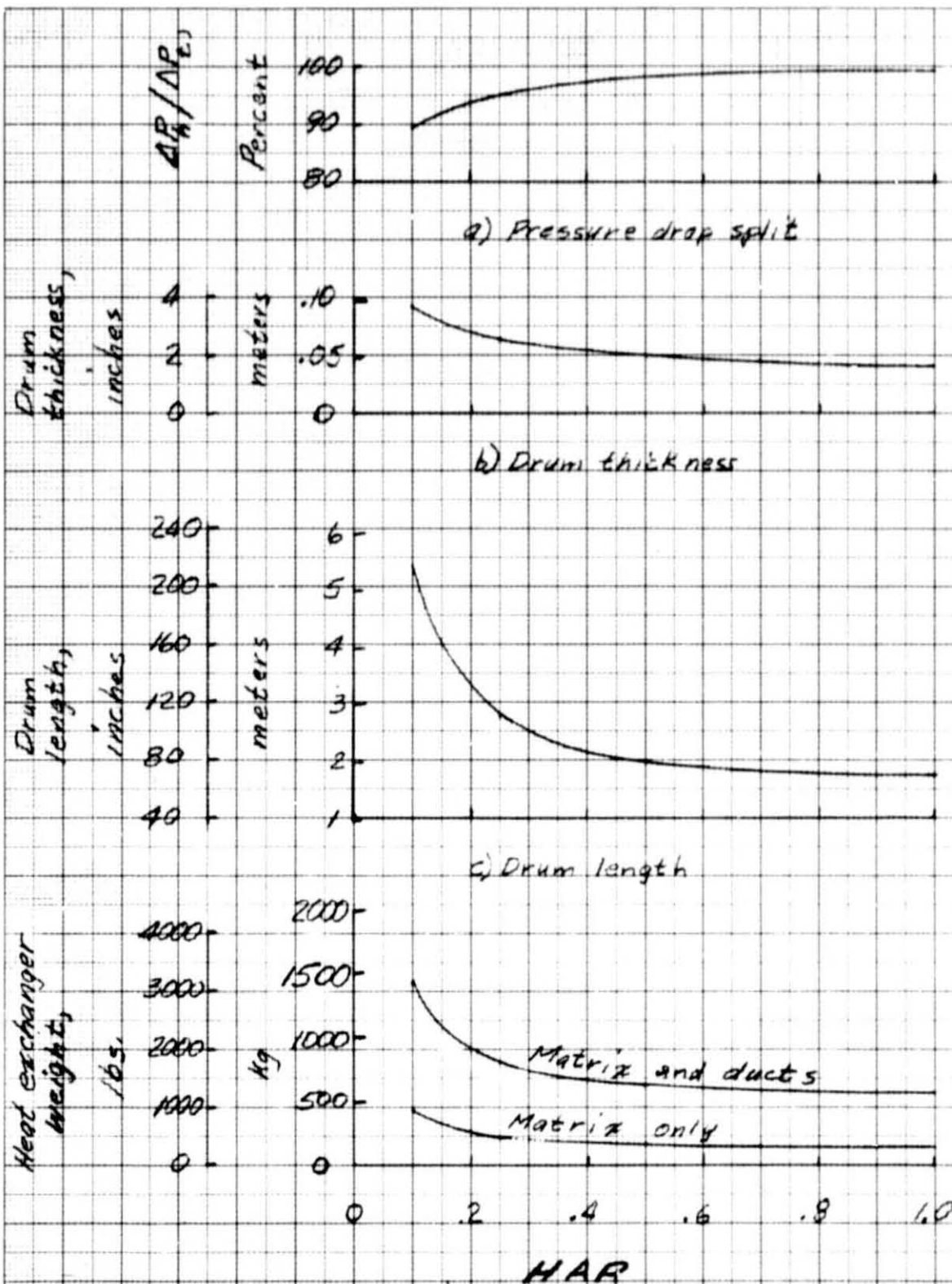


c) Drum length



d) Engine weight

Figure 9. - (concluded)



d) Weight of heat exchanger

Figure 10. - General heat exchanger trends versus HAR.
 $E=0.90$, $\Delta P_h=8$ percent, $OPR=12$, $FPR=1.6$, $BPR=9$, $T_h=1700K$,
 Mach 0.80, 10.67km (35000ft), drum diameter fixed.

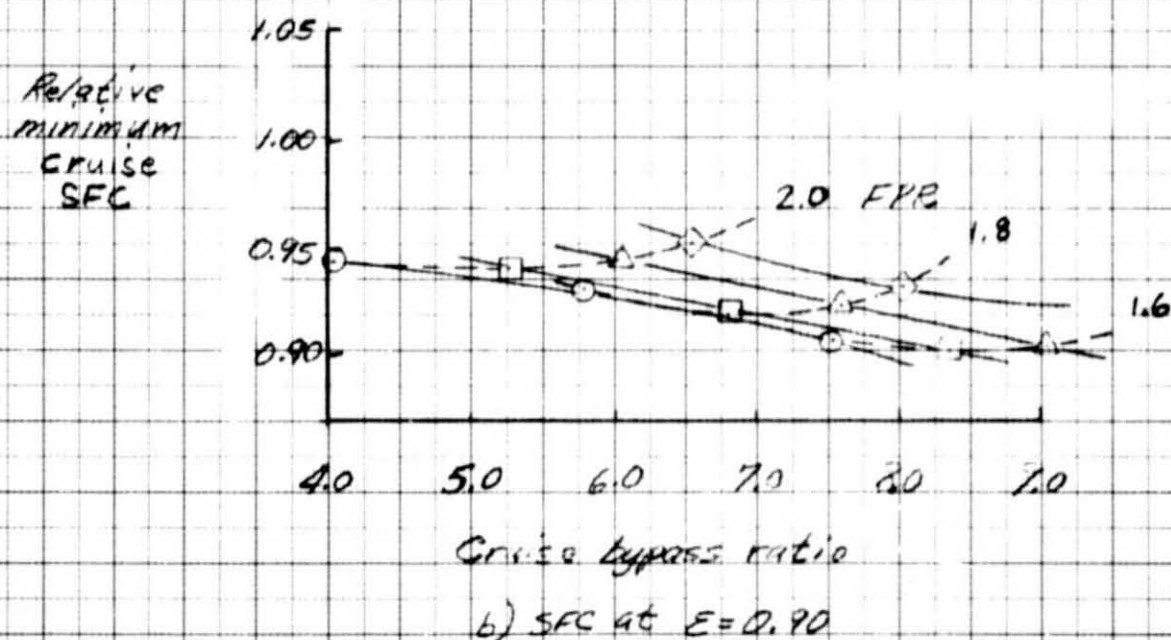
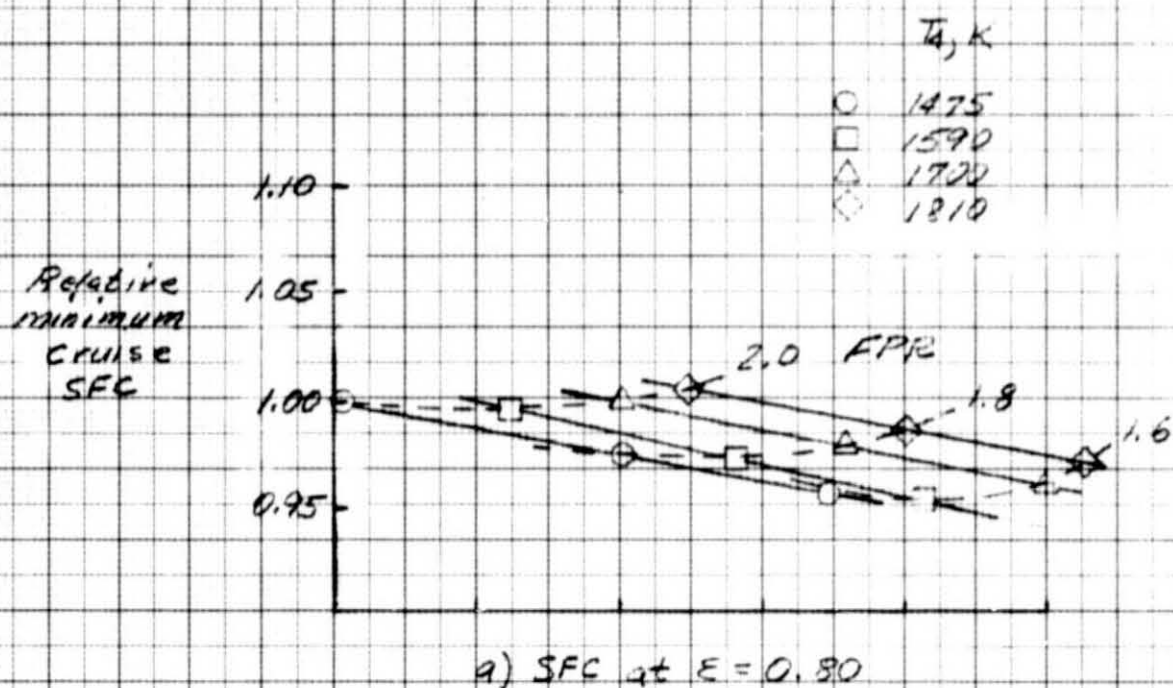


Figure 11. - Relative minimum SFC versus bypass ratio for several FPR's and T_4 's. $E = .80$ and $.90$, $OPR = 10$, $\Delta P_t = 12$ percent.

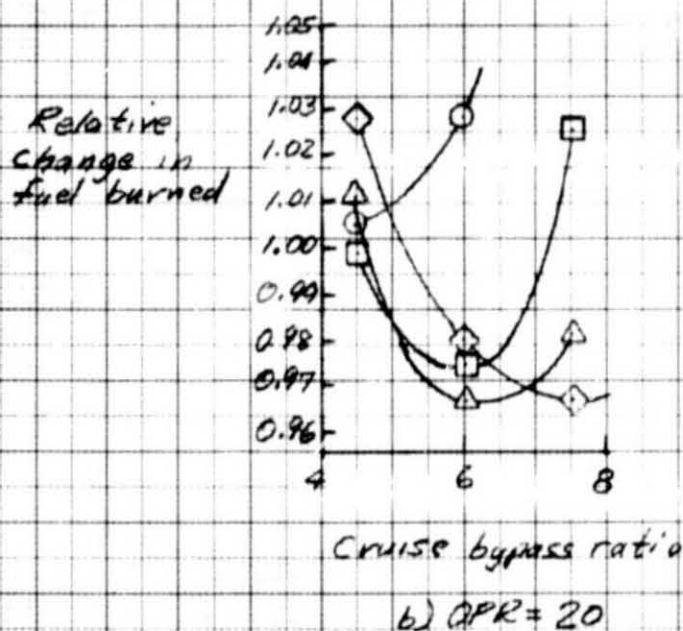
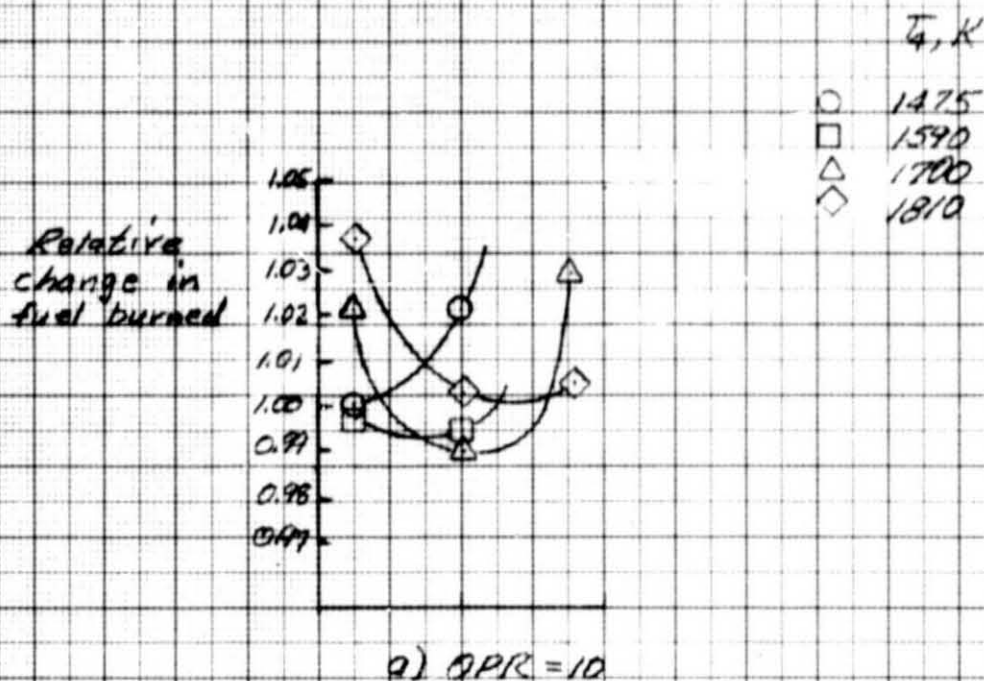
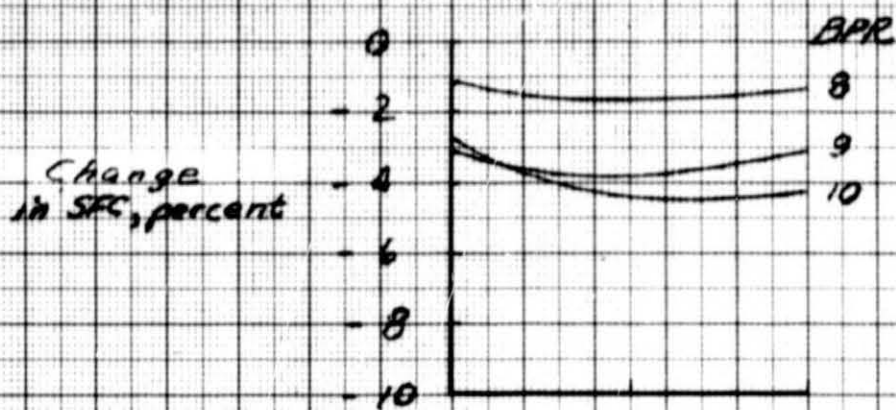
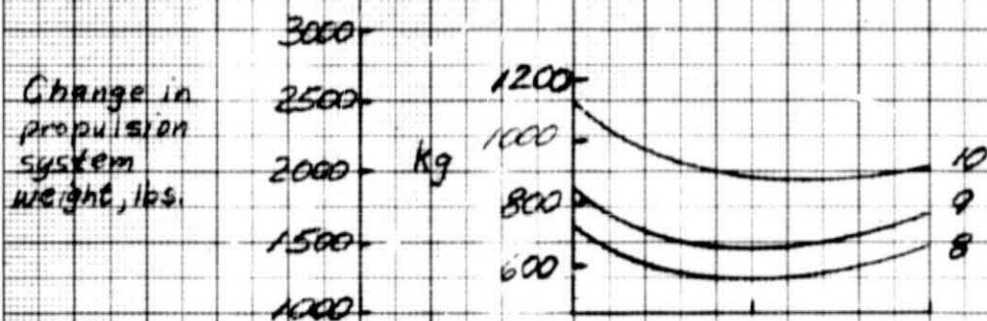


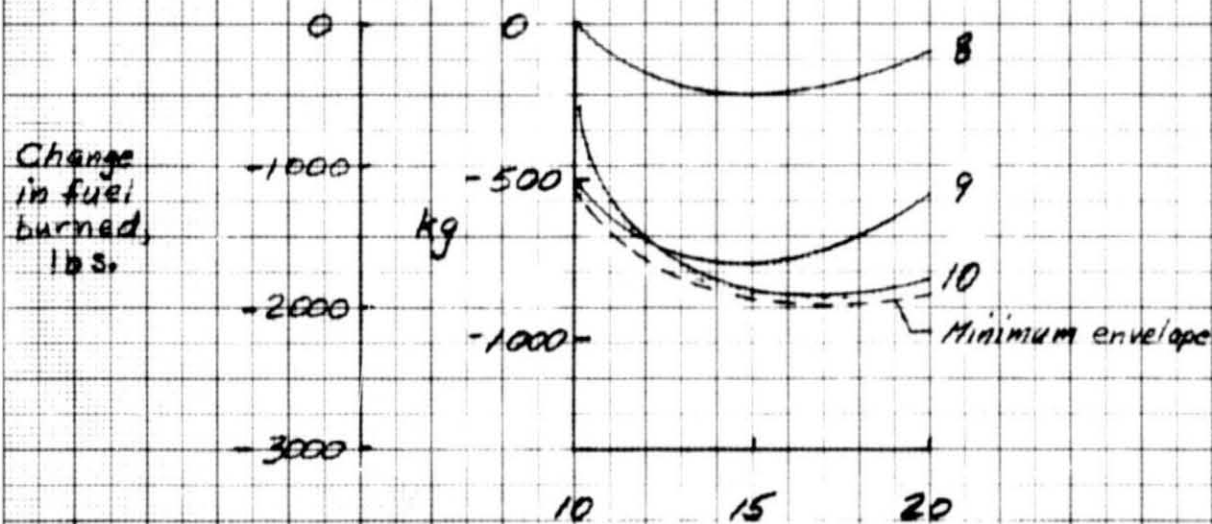
Figure 12 - Relative change in fuel burned versus bypass ratio for several levels of T_4 .
 $\epsilon = 0.80$, $APR = 12$ percent.



a) SFC

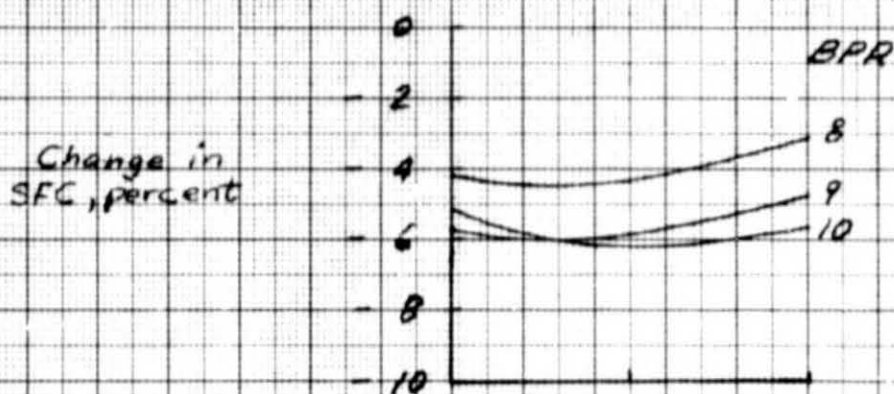


b) Weight

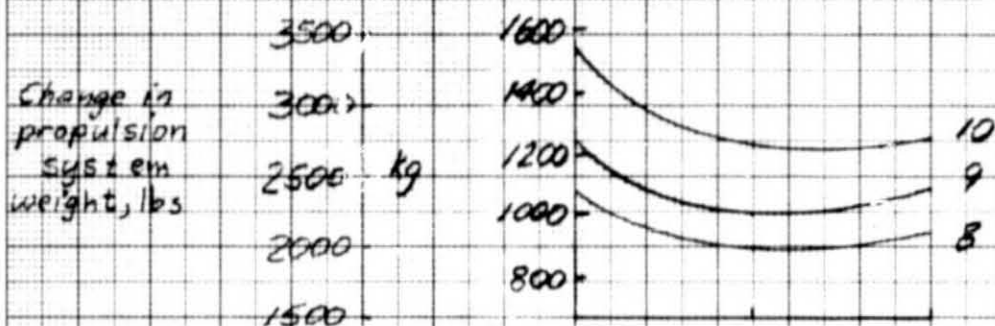


c) Fuel burned

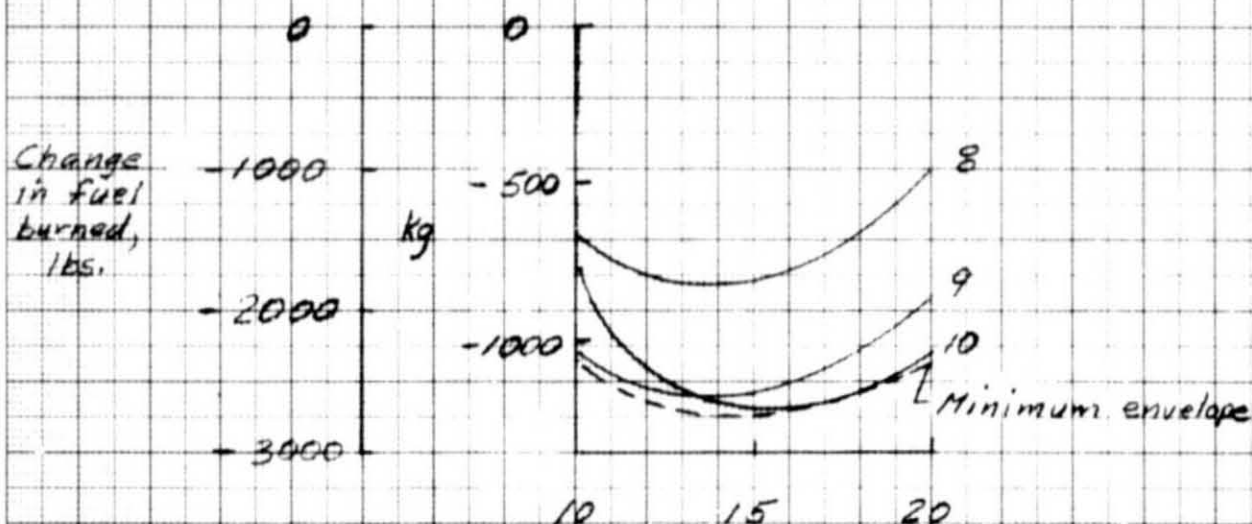
Figure 13. - SFC, engine weight, and change in fuel burned versus OPR. $E=0.80$, $\Delta P_c=4$ percent, $T_4=1700K$, $FPR=1.6$, altitude = 10.67 km, Mach 0.80.



a) SFC



b) Weight



c) Fuel burned

Figure 1d.- SFC, engine weight, and change in fuel burned versus OPR. $\epsilon = 0.85$, $\Delta P_e = 4$ percent, $T_4 = 1700K$, FPR = 1.6, altitude = 10.67 km, Mach = 0.80.

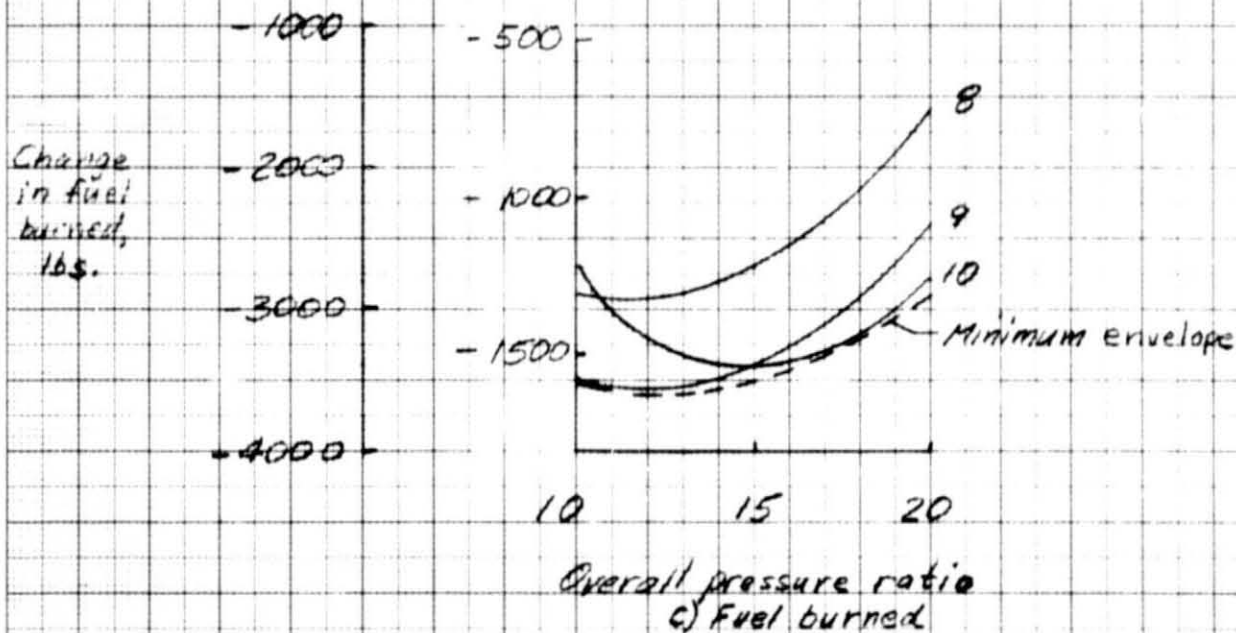
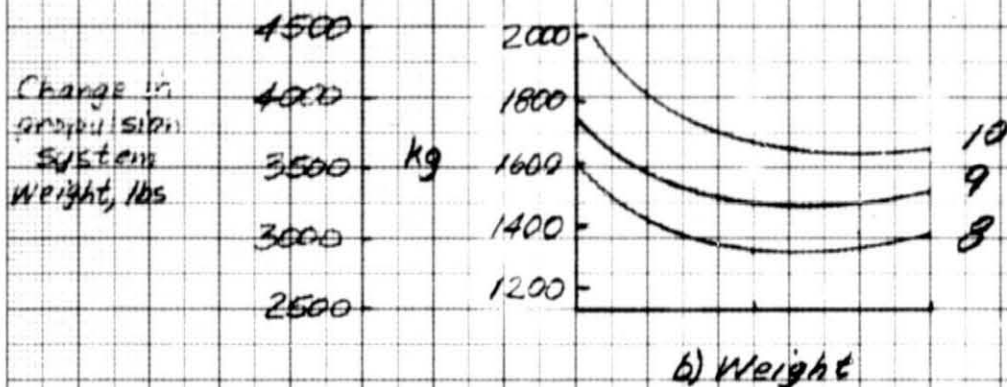
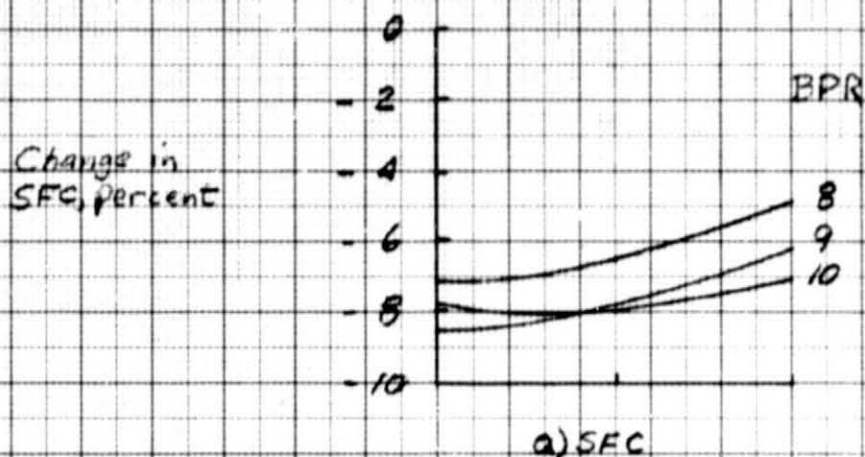
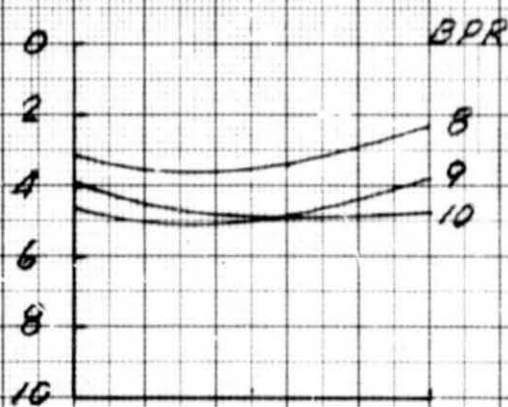


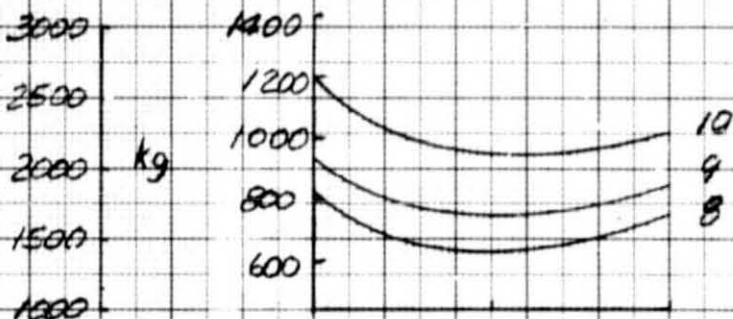
Figure 15.- SFC, engine weight, and change in fuel burned versus OPR. $E=0.80$, $\Delta P_2=4$ percent, $T_4=1700K$, $FPR=1.6$, altitude = 10.67 km, Mach = 0.80.

Change in
SFC, percent



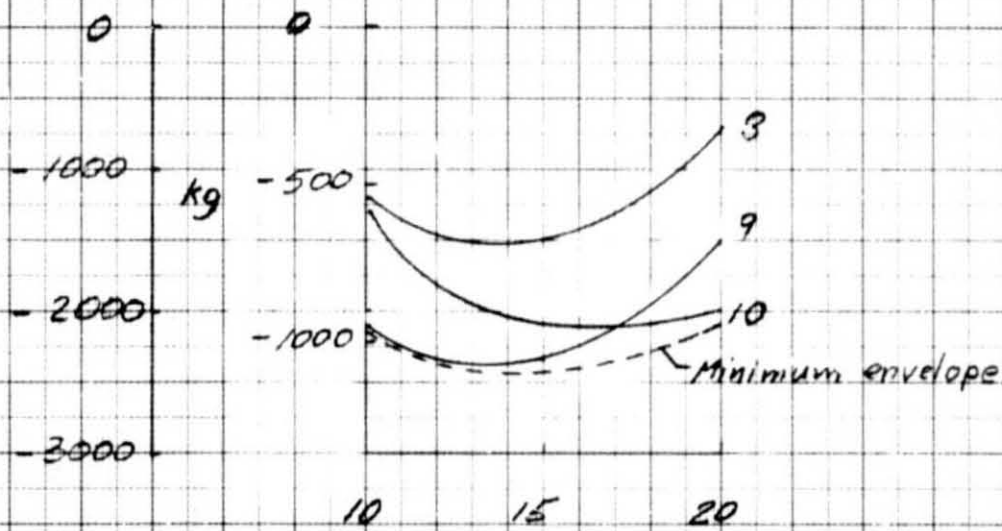
a) SFC

Change in
propulsion
system
weight, lbs



b) Weight

Change
in fuel
burned,
lbs.



Overall pressure ratio
c) Fuel burned

Figure 16.- SFC, engine weight, and change in fuel burned versus OPR. $E=0.85$, $\Delta P_t=2$ percent, $T_4=1700K$, $FPR=1.6$, altitude = 10.67 km, Mach = 0.80.

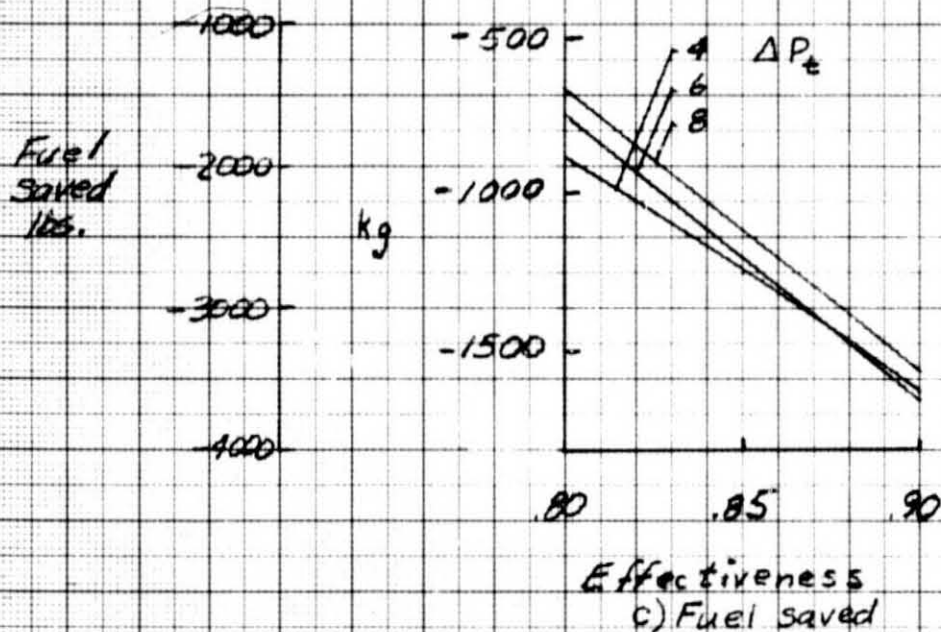
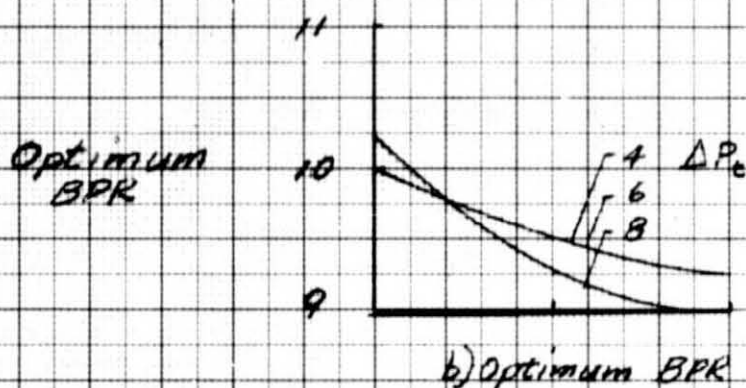
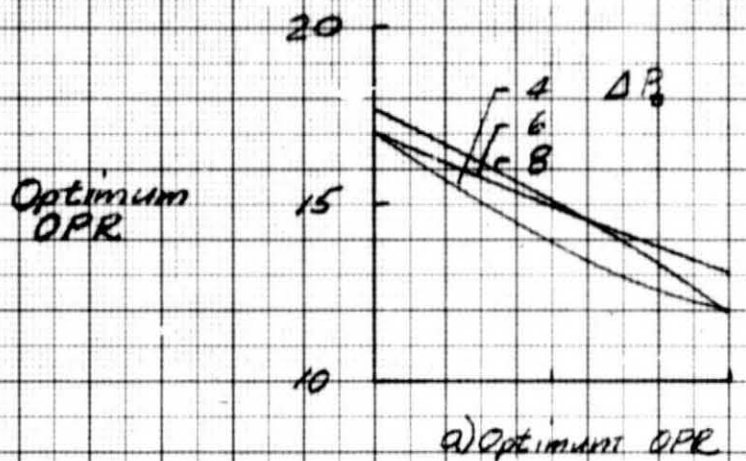


Figure 17.- Optimum engine parameters and fuel saved versus ϵ for several values of ΔP_e . $T_0=1700^\circ\text{K}$, $FPR=1.6$, altitude = 10.67 km, Mach = 0.80, no drag effects due to changing engine size. No leakage or carry over losses.

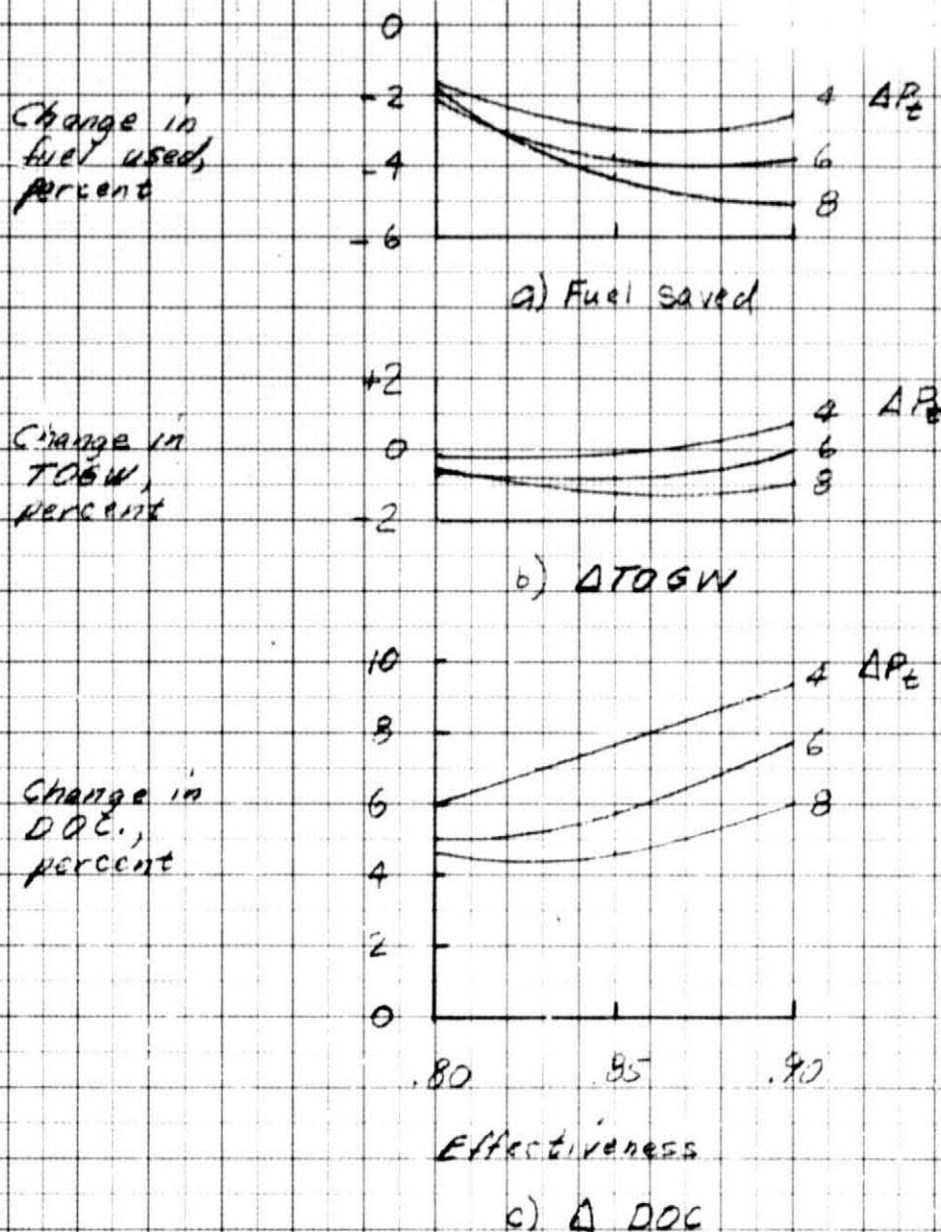


Figure 18.- Fuel saved, $\Delta TOGW$, and ΔDOC versus E
 The nine best engines including drag effects.
 No leakage or carry over losses

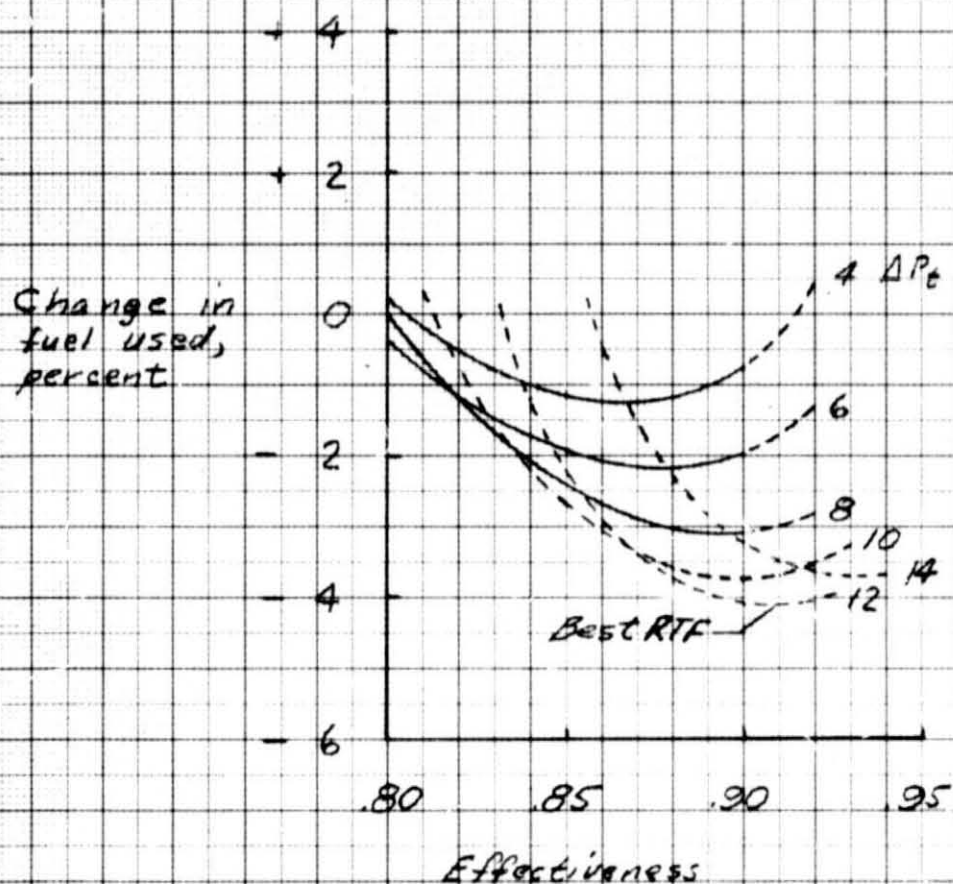


Figure 19.- Fuel saved by regenerative turbofan engines compared to the reference advanced turbofan. Included is the effect of leakage and carry over losses of 2 and 1 percent respectively, and the drag effect.

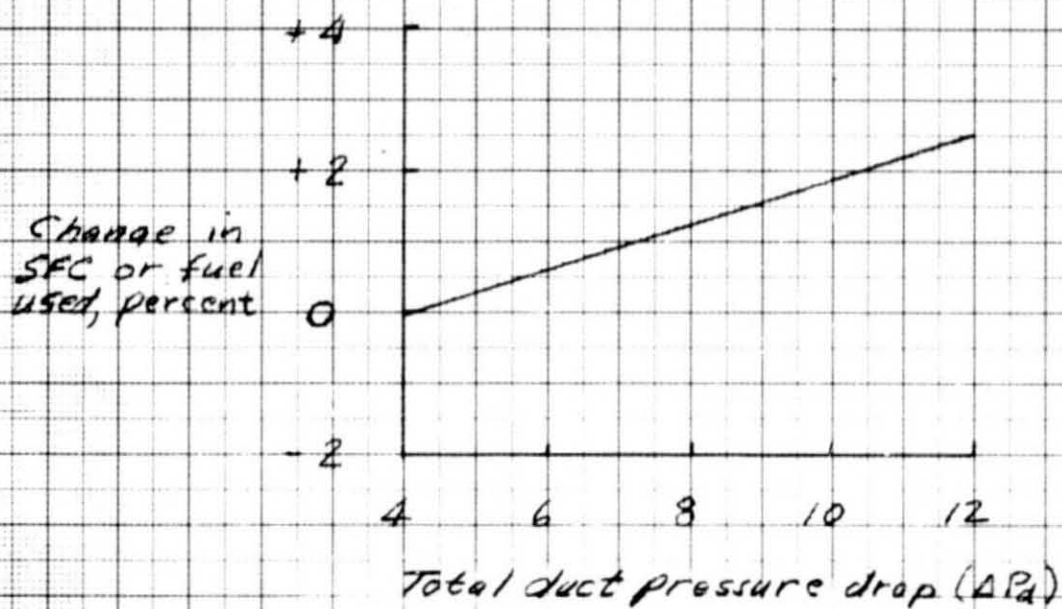


Figure 20.- The effect of ΔP_d on SFC

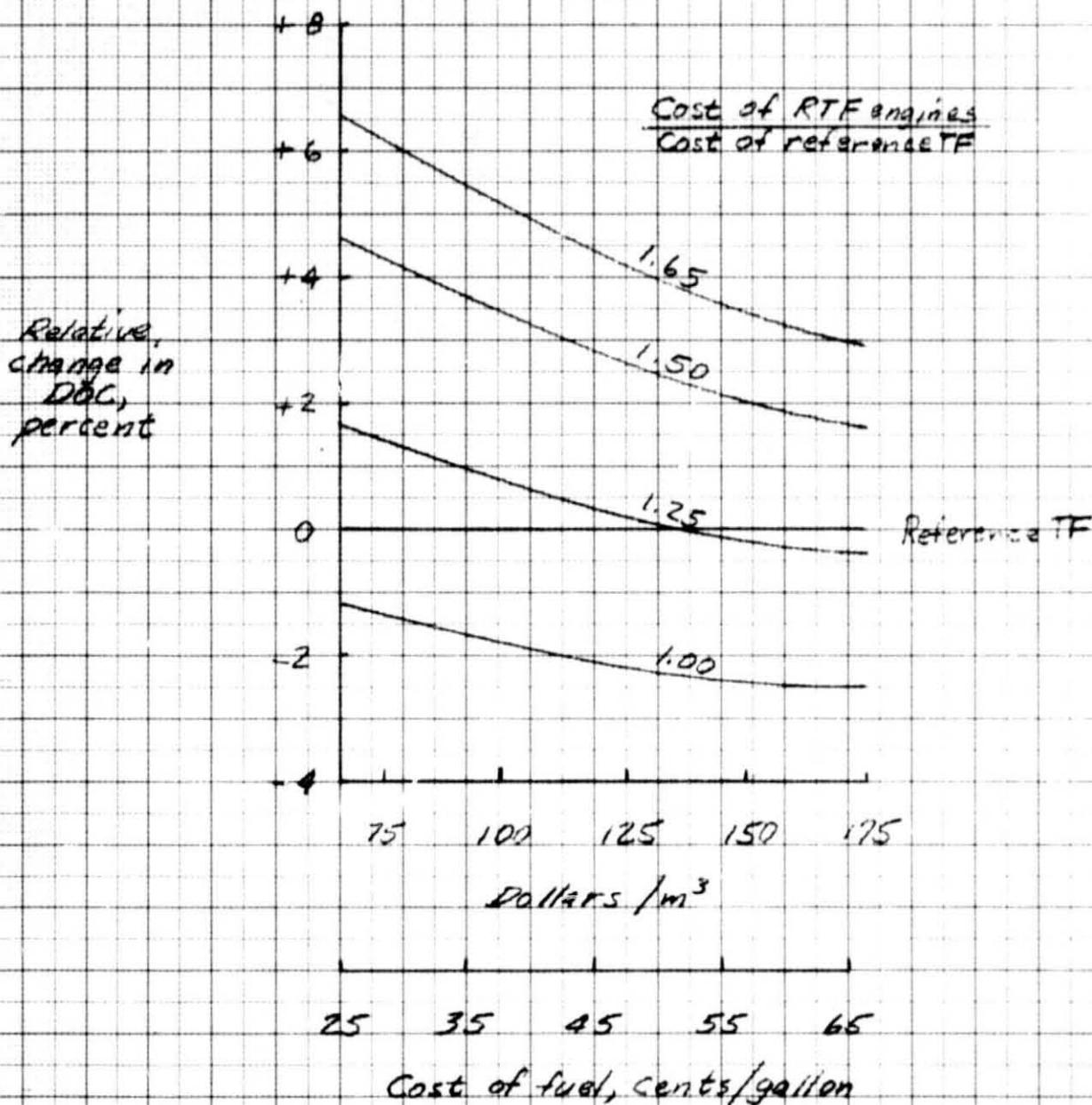


Figure 21.- Percent change in DOC versus fuel cost for several levels of engine cost relative to a reference turbofan.
 Best RTF, $AP_0 = 8$ percent, $E = 90$, $QPR = 12$, $BPR = 9$, $HAR = .70$,
 $T_0 = 1700K$, $FPR = 1.6$, Leakage 2 percent, Carry over 1 percent,
 $Mach = 0.80$, altitude ≈ 10.67 km (35000 ft).